Yamaceratops Dorngobiensis, a New Primitive Ceratopsian (Dinosauria: Ornithischia) from the Cretaceous of Mongolia

Authors: MAKOVICKY, PETER J, and NORELL, MARK A

Source: American Museum Novitates, 2006(3530) : 1-42

Published By: American Museum of Natural History

URL: https://doi.org/10.1206/0003-0082(2006)3530[1:YDANPC]2.0.CO;2

AMERICAN MUSEUM
Novitates

PUBLISHED BY THE AMERICAN MUSEUM OF NATURAL HISTORY
CENTRAL PARK WEST AT 79TH STREET, NEW YORK, NY 10024
Number 3530, 42 pp., 20 figures September 08, 2006

Yamaceratops dorngobiensis, a New Primitive Ceratopsian (Dinosauria: Ornithischia) from the Cretaceous of Mongolia

PETER J. MAKOVICKY[1] AND MARK A. NORELL[2]

ABSTRACT

A new basal neoceratopsian taxon from the eastern Gobi Desert is described. *Yamaceratops dorngobiensis*, tax. nov., is probably of late Early Cretaceous age, and occupies a phylogenetic position intermediate between *Liaoceratops* and *Archaeoceratops*. It is the most basal taxon to display a number of traditional neoceratopsian synapomorphies concentrated in the cheek region and mandible. These include presence of an epijugal, lateral displacement of the coronoid process, a lateral ridge on the surangular for insertion of the jaw adductors, and a lateral wall to the mandibular glenoid. *Yamaceratops* shares two synapomorphies (tubercles on the ventral edge of the angular and shape of the jugal) with *Liaoceratops*, indicating that the transient presence of derived characters may be prevalent in the early evolutionary history of Ceratopsia. *Yamaceratops* shares aspects of frill morphology with *Liaoceratops* and *Leptoceratops* that suggest a function unrelated to display for this anatomical structure in basal neoceratopsians, and hints at a more complex evolutionary history for ceratopsian frills. Considerations of patristic distances and mosaic evolution among basal neoceratopsian taxa indicate that a greater diversity of these animals remains undiscovered.

INTRODUCTION

In spite of an implied ghost lineage for most of the Early and early Late Cretaceous, unquestionable neoceratopsian fossils were unknown for this period until the recent discovery of *Archaeoceratops* from the Late Albian of China (Dong and Azuma, 1997). Since then, several new Early Cretaceous neoceratopsian specimens have been reported, including the basal form *Liaoceratops* (Xu et al., 2002) and an enigmatic basal taxon

[1] Department of Geology, The Field Museum, 1400 S. Lake Shore Drive, Chicago IL 60605 (pmakovicky@fieldmuseum.org).
[2] Division of Paleontology, American Museum of Natural History (norell@amnh.org).

 ISSN 0003-0082

Chaoyangsaurus (Zhao et al., 1999) based on a holotype that was found several decades ago, but remained undescribed until recently. Cladistic analyses by Sereno (1999, 2000), You and Dodson (2003), and Chinnery (2004) found *Chaoyangsaurus* to be a neoceratopsian, but the systematic position of this taxon has been contested, and Makovicky (2001) and Xu et al. (2002) posited this taxon to lie outside of the neoceratopsian–psittacosaurid clade. The age of *Chaoyangsaurus* has also been the subject of debate. Whereas Zhao et al. (1999) attributed a Middle to Late Jurassic age for the Tuchengzhi Formation from which the holotype derives, more recent radiometric dates from near the top of that formation yielded a date of 139 MYA (Swisher et al., 2002), demonstrating that this formation extends into the earliest Cretaceous. In sum, only two taxa, *Liaoceratops* and *Archaeoceratops*, are widely recognized as Early Cretaceous neoceratopsians, in contrast to the 36 or so valid taxa known from the last two stages of the Cretaceous. This disparity belies a still unsampled diversity of taxa at the base of Neoceratopsia.

The 1991 American Museum of Natural History–Mongolian Academy of Sciences (hereafter AMNH-MAS) expedition explored Cretaceous fossil localities in the eastern part of the Gobi Desert, Dorngobi Aimag, Mongolia. A small ceratopsian skull was collected from reddish, poorly consolidated sandstones at the Khugenetslavkant locality. In 2002 and 2003, members of the AMNH-MAS expeditions returned to this locality and collected more ceratopsian material, including a specimen comprising associated skull and skeletal elements. These materials represent a new basal neoceratopsian taxon, which is described here. Where applicable, spelling of Mongolian place names follows Benton (2000) with variant spellings provided in parentheses.

Institutional Abbreviations

AMNH, American Museum of Natural History, New York; BMNH, The Natural History Museum, London; IGCAGS, Institute of Geology Chinese Academy of Geosciences, Beijing; IGM, Institute of Geology Mongolia, Ulanbaatar; IVPP, Institute of Vertebrate Paleontology and Paleoanthropology, Beijing; MOR, Museum of the Rockies, Bozeman; CMN, Canadian Museum of Nature, Ottawa; PIN, Paleontological Institute, Moscow; TsNIGRI, Chernyshev's Central Museum of Geological Exploration, St. Petersburg; TMP, Royal Tyrrell Museum of Palaeontology, Drumheller; USNM, United States National Museum, Washington DC; ZPAL, Institute of Paleobiology, Polish Academy of Sciences, Warsaw.

SYSTEMATIC PALEONTOLOGY

ORNITHISCHIA MARSH, 1890

CERATOPSIA MARSH, 1890

NEOCERATOPSIA SERENO, 1986

Yamaceratops dorngobiensis, new taxon

Etymology: The genus is named for Yama, a Tibetan tantric Buddhist deity, who is the Lord of Death and one of the eight Dharmapalas, or protectors, of Buddhist teaching. Yama has the head of a water buffalo and bears horns, a trait from which ceratopsians derive their name. The specific name refers to the Eastern Gobi provenance of this taxon.

Locality and Geological Setting: The specimen derives from a fluvial, pale red sandstone layer at Khugenetslavkant. These redbeds appear to overlie the Khar Khutul (= Khar Hötöl) beds and underlie an unnamed unit with a fauna of segnosaurs, advanced iguanodontians, and ornithomimosaurs reminiscent of the Iren Dabasu fauna (Gilmore, 1933; Currie and Eberth, 1993). The Khar Khutul beds may be correlated with the Khuren Dukh (= Hüren Dukh) beds that have been interpreted as Aptian–early Albian in age (Jerzykiewicz and Russell, 1991; Khand et al., 2000), but have also been dated as Barremian (~128 MYA) by Shuvalov (2000). The age of the Iren Dabasu fauna has been poorly constrained with ages ranging from the Cenomanian to the early Campanian (Jerzykiewicz and Russell, 1991; Currie and Eberth, 1993; Khand et al., 2000). If the correlations outlined above are correct,

the Khugenetslavkant sandstone facies appears to be late Early Cetaceous in age. This is roughly similar or perhaps slightly younger than the Albian age ascribed to *Archaeoceratops* (Tang et al., 2001). Stratigraphic relationships among central Asian continental sediments are still poorly understood and much work remains to be done in this respect.

DIFFERENTIAL DIAGNOSIS: Small basal ceratopsian taxon with unkeeled rostral unlike all other Neoceratopsia (optimization-dependent unique trait); rostral patterned with anastomosing ridges and grooves (present in neoceratopsians more derived than *Liaoceratops*); subtemporal part of jugal lobate and deeper than suborbital section (plesiomorphic for Neoceratopsia, shared only with *Liaoceratops*); epijugal ossification present (plesiomorphic for neoceratopsians other than *Liaoceratops*); angular with two tubercles along ventral edge (unique trait; three tubercles present in *Liaoceratops*); surangular forming vertical wall to glenoid (plesiomorphic for neoceratopsians more derived than *Liaoceratops*); all cheek teeth with distinct, offset primary ridge (plesiomorphic for neoceratopsians more derived than *Liaoceratops*).

HOLOTYPE: The holotype (IGM 100/1315) consists of a partial skull missing the premaxillae, rostral, and predentary, as well as much of the frill and the left cheek and posterior part of the left mandible. The holotype skull appears to be from a mature individual, as witnessed by closure of the sutures among the occipital and basicranial braincase elements. The epijugal is not fused to the jugal, a feature that appears to be related to advanced maturity in *Protoceratops andrewsi* and ceratopsids. The skull is only dorsoventrally compacted to a small degree.

REFERRED MATERIALS: A referred specimen (IGM 100/1303) collected in 2002 comprises the rostral, left maxilla, right jugal and quadrate, the left surangular, both articulars, a few isolated teeth, three partial vertebrae, the left ilium, and several hindlimb fragments. Additionally, a large number of fragmentary ceratopsian bones were surface collected from the Khugenetslavkant locality by the 2002 and 2003 AMNH-MAS field crews. An isolated predentary, IGM 100/1867, is described here and can safely be referred to *Yamaceratops* based on its similarity with the predentaries of other basal neoceratopsians.

DESCRIPTION

OPENINGS OF THE SKULL: The bones that circumscribe the naris are missing from both the holotype and the referred specimen (figs. 1–3). The antorbital fossa is subtriangular in outline, but does not extend as far below the anterior margin of the orbit as in the holotype of *Archaeoceratops* (IVPP V11114). At its ventral end, the fossa forms a deep pocket in the body of the maxilla above and lateral to the tooth row (fig. 2). The dorsal half of the fossa is recessed into the lacrimal, which meets the maxilla in an oblique suture along the floor of the fossa (fig. 1). Neither specimen preserves the rim of the antorbital fenestra, which is highly reduced in most ornithischians.

As in other ceratopsians, the orbit is circumscribed by the jugal, lacrimal, prefrontal, the frontal, and postorbital (figs. 1–3). The jugal forms the entire ventral orbital rim, which is shallowly concave. Anteriorly, the jugal bears a short spur that overlaps the base of the lacrimal and forms a distinct angle at the anteroventral corner of the orbit (fig. 1). A similar spur occurs in *Archaeoceratops* (IVPP V11114), *Protoceratops* (AMNH 6429, 6466), *Leptoceratops* (CMN 8887, 8889), and some other ceratopsians. The lacrimal forms only a small part of the anterior rim of the orbit, which is mainly bounded by the prefrontal. The frontal contribution is relatively short and bridges the small gap between the prefrontal and the rostral process of the postorbital (fig. 3). The postorbital provides the largest single contribution to the orbit. The posterodorsal corner of the orbit is formed at the intersection of the short rostral process and the long descending process, which bounds the entire posterior rim.

Both the infratemporal and supratemporal fenestrae are preserved only on the right side of the holotype (figs. 1, 3). As in other basal neoceratopsians, the postorbital is excluded from the margin of the infratemporal fenestra by the long dorsal process of the jugal. The subtemporal portion of the jugal is relatively deep and the ventral border of the fenestra is

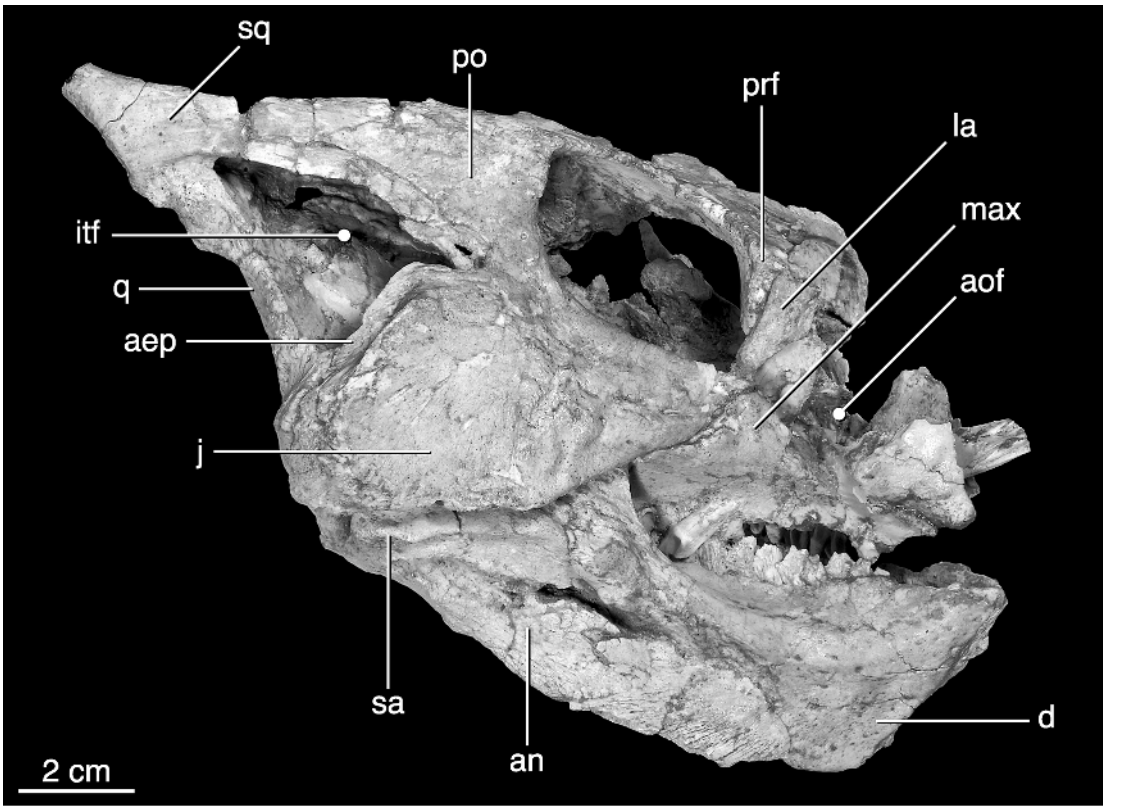

Fig. 1. Left lateral view of the holotype skull of *Yamaceratops dorngobiensis* (IGM 100/1315). Abbreviations are explained in appendix 3.

level with the ventral-most point of the orbit. A small embayment in the jugal border of the fenestra, adjacent to the ventral end of the postorbital, is observed on the right side of the specimen (fig. 1). This embayment appears to have finished edges and is not observed in any other basal ceratopsian taxon. It may be a unique feature in this individual, perhaps due to pathology, or may represent a derived character of *Yamaceratops*.

The supratemporal fenestra is only partially preserved because most of the frill is missing in the holotype. The rostral end of the fenestra extends as a shallow depression on to the caudal edge of the frontal (fig. 3). Laterally, the postorbital overhangs the fenestra and does not form a shelf along the fenestral edge as in *Leptoceratops* (CMN 8887, 8889), *Montanoceratops* (Makovicky, 2001), and an undescribed leptoceratopsid specimen from Alberta (TMP 88.11.1; Ryan and Currie, 1998). The anterior edge of the fenestra forms a wide concave curve and is not constricted in dorsal view.

ROSTRAL: The rostral of IGM 100/1303 is nearly complete, missing only part of the buccal margin and the left buccal process (fig. 4). The rostral is relatively thick compared to the other skull bones, and it has a rugose, highly vascularized outer texture traversed by anastomosing grooves (fig. 4A), a feature seen in most other neoceratopsians except for *Liaoceratops*. Although it is more acutely U-shaped in ventral view than the rostral of psittacosaurs (i.e., AMNH 6542), the rostral of *Yamaceratops* is not sharply keeled as in more advanced neoceratopsians. Dorsally, the rostral bears a slender process that would have wedged between the two halves of the premaxillary internarial bar. This process continues as a thin midline crest about halfway down the internal surface of

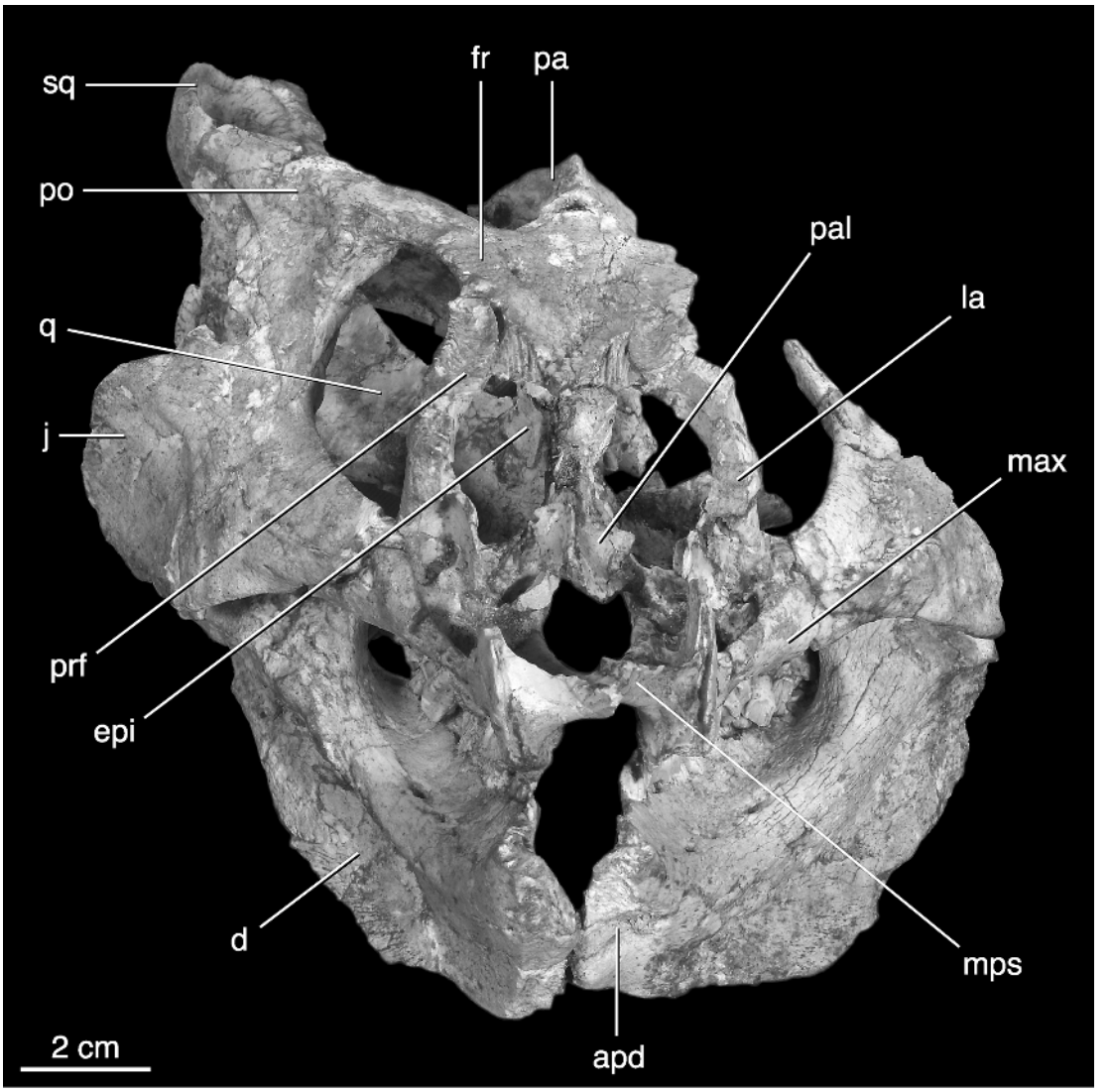

Fig. 2. Rostral view of the holotype skull of *Yamaceratops dorngobiensis* (IGM 100/1315). Abbreviations are listed in appendix 3.

the rostral (fig. 4B). A similar crest is present on the internal midline of the rostral of *Brachyceratops* (Gilmore, 1917; USNM 8072, USNM 14765) and is more prominent on the smaller juvenile rostral (USNM 8072) than on the larger one (USNM 14765). It is probably a widespread feature among neoceratopsians, but its presence is often concealed by the articulated nature of specimens.

The right buccal (lateral) process is preserved, but appears to be incomplete caudally (fig. 4). It is grooved dorsally where it fits onto the ventral edge of the premaxilla. The preserved buccal margin appears relatively blunt, which suggests that the cropping edge was formed entirely by a thick keratinous beak. A buccal process was proposed as a potential synapomorphy uniting leptoceratopsids with Ceratopsidae to the exclusion of

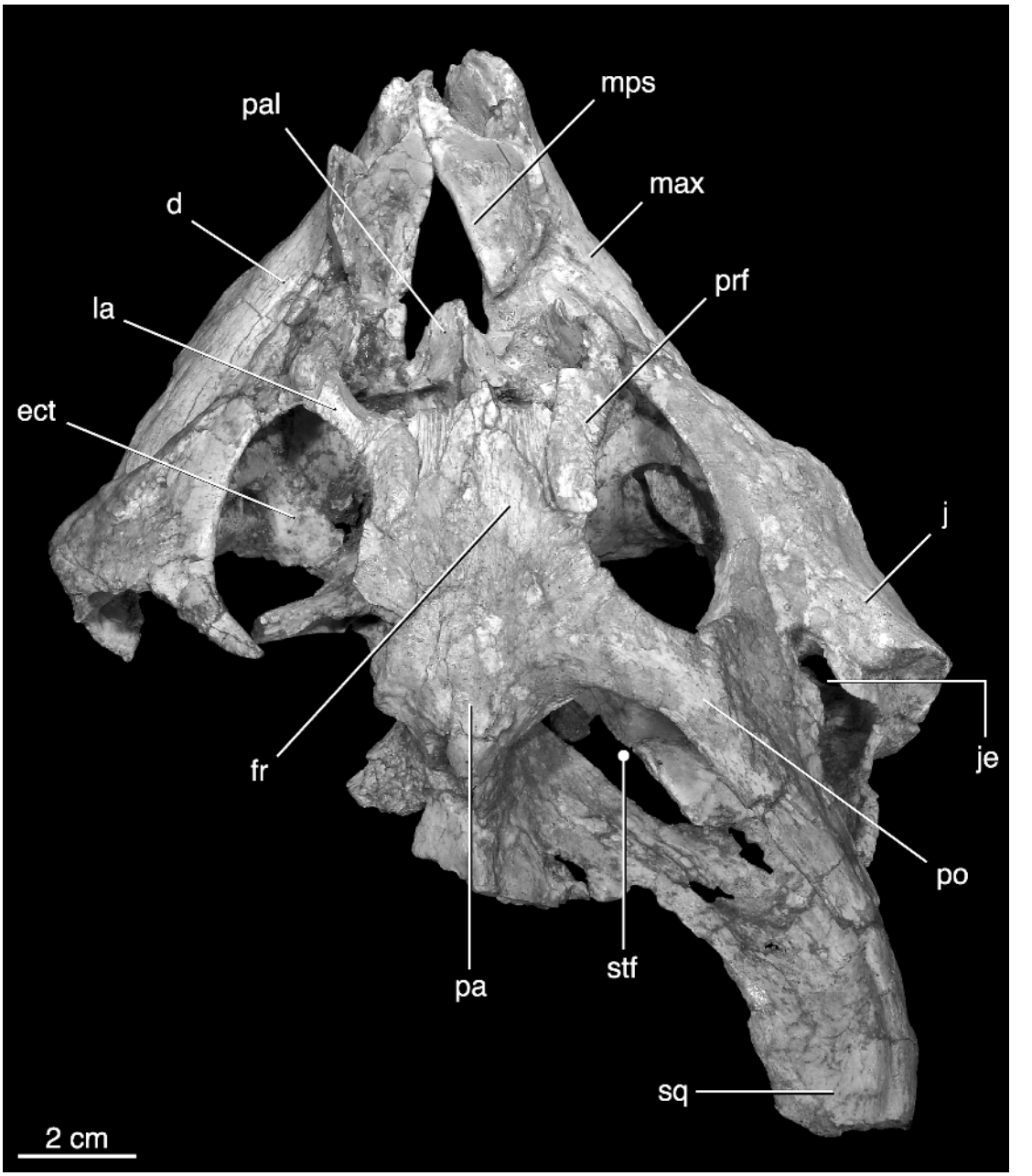

Fig. 3. Dorsal view of the holotype skull of *Yamaceratops dorngobiensis* (IGM 100/1315). Abbreviations are listed in appendix 3.

other neoceratopsians by You and Dodson (2003). As demonstrated in *Yamaceratops*, this character has a broader distribution and is present in all neoceratopsian taxa that preserve the rostral, including *Liaoceratops*. Sereno (2000) and You and Dodson (2003) regarded this structure as absent in *Protoceratops*, but juvenile specimens of *Protoceratops* sp. from Ukhaa Tolgod reveal that it is present as a differentiated process in

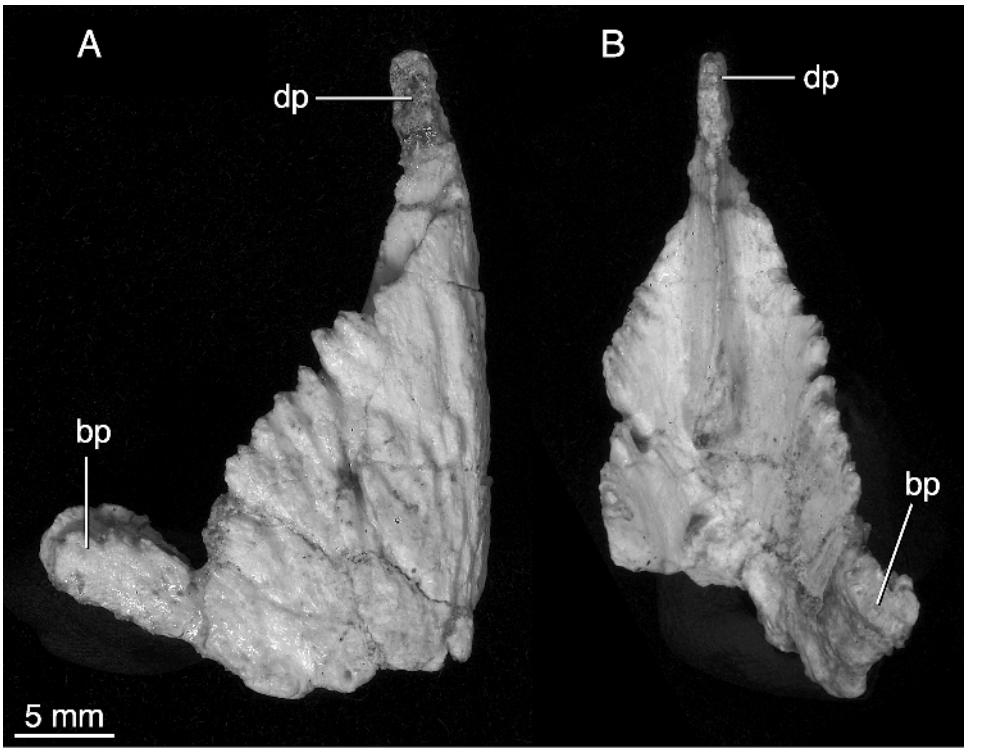

Fig. 4. Rostral bone of the referred specimen of *Yamaceratops dorngobiensis* (IGM 100/1303) in lateral (**A**) and internal (**B**) views. Abbreviations are listed in appendix 3.

ontogenetically young individuals, and its apparent absence is related to expansion of the lateral sheet of bone between the buccal and dorsal processes through ontogeny.

MAXILLA: The maxilla is a complex bone, which forms the majority of the preorbital portion of the face. Rostrally, the body of the maxilla meets the premaxilla along a straight, but oblique, suture near the buccal margin (figs. 1, 5A). Neither the holotype nor the referred specimen preserves the dorsal edge of the maxilla where it would meet the nasal and lacrimal. The maxilla bears a long rostral process that extends forward to form the palate between the premaxillae (figs. 2, 5), which were apparently excluded from the palate as in other marginocephalians (Sereno, 1986). The rostral process is triangular in cross section with a vertical midline sutural surface where it meets its counterpart anterior to the choana. The sutural surface is marked by a series of horizontal, parallel striations in the disarticulated maxilla of IGM 100/1303 (fig. 5B); these would have interlocked with striations from the opposite maxilla. The roof of the palatal shelf is dorsally concave (fig. 3). Posterior to the maxillary palatal roof, the palatal shelves diverge and form an elongate spindle-shaped choanal vacuity between them (fig. 3) as in other basal neoceratopsians (Osmólska, 1986). The maxilla meets the palatine along an oblique suture on the palate as in most ornithischians.

The body of the maxilla widens caudally beneath the antorbital fossa. Above the tooth row, the face of the maxilla curves laterally to form a deep "cheek" recess lateral to the tooth row, but there is no sharp crest as in some basal ornithopods (fig. 5A). The floor of the antorbital fossa is excavated by a deep pocket, which appears to end just dorsal and lateral to the tooth roots in the holotype. The tooth row is partially preserved in both maxillae of the holotype, as well as in the left maxilla of the referred specimen. There are about 11 or 12

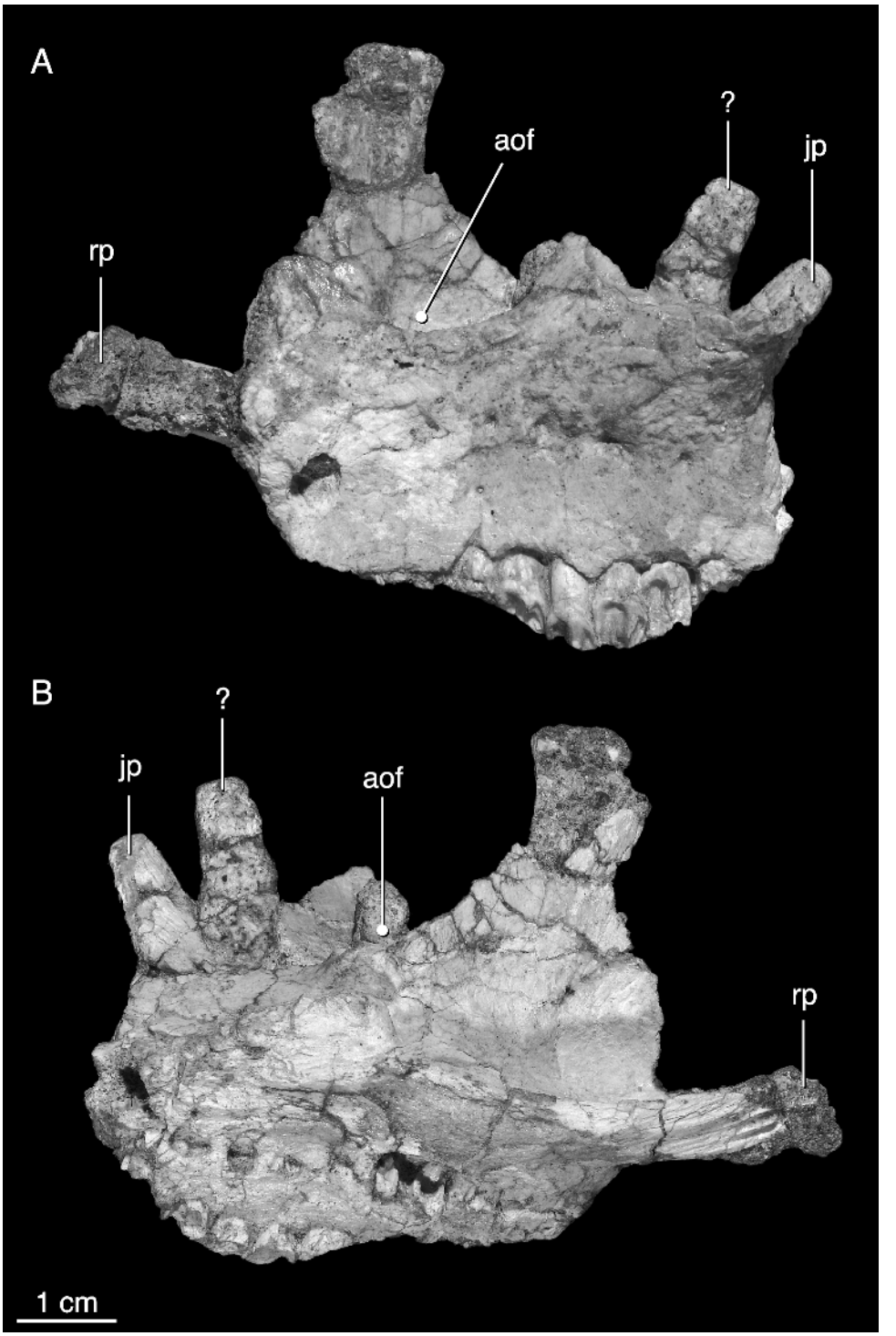

Fig. 5. Left maxilla of the referred specimen of *Yamaceratops dorngobiensis* in lateral (**A**) and medial (**B**) views. Abbreviations are listed in appendix 3.

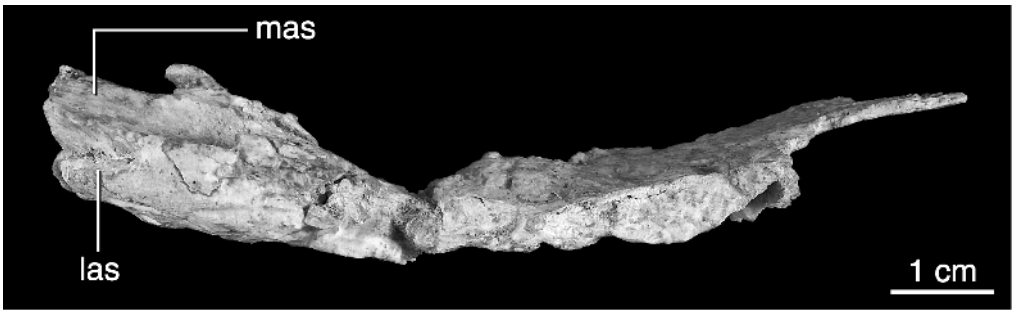

Fig. 6. Right partial jugal of the referred specimen of *Yamaceratops dorngobiensis* (IGM 100/1303) in dorsal view, showing details of the maxillary articulation on rostral end. Abbreviations are listed in appendix 3.

tooth positions in both the holotype and the referred specimen, representing a number similar to *Liaoceratops* (Xu et al., 2002) and *Archaeoceratops* (You and Dodson, 2003).

Caudally, the maxilla has a complex articulation with the jugal, the details of which are best seen in the disarticulated referred specimen (figs. 5, 6). Laterally, the concave caudal end of the maxilla slots onto the anterior end of the jugal along a curved and oblique suture that extends from the caudal wall of the antorbital fossa to below the orbit (fig. 5A). Adjacent to this facial process, the medial edge of the maxilla bears a long fingerlike process, which slots into a groove on the medial face of the jugal (fig. 5B). A third apparent process just rostral to the medial process (fig. 5A) is actually a separate piece of bone adhering to the maxilla, perhaps derived from the lacrimal.

The anatomy of the jugal–maxillary contact is difficult to evaluate in a majority of basal ceratopsians, either because the elements remain in tight articulation (*Leptoceratops* 8887, 8889; most specimens of *Protoceratops* and *Bagaceratops*; *Archaeoceratops* IVPP V11114; *Liaoceratops* IVPP V12738) or are abraded or missing as in *Montanoceratops* (AMNH 5464). Disarticulated specimens reveal a broad overlapping suture in *Montanoceratops* (MOR 542), *Protoceratops* (IGM 100/1130), and *Prenoceratops* (Chinnery, 2004). In *Udanoceratops* (PIN 3907/11) the maxilla bears a robust jugal process that is triangular in cross section and which fits into a wide slot on the medial face of the jugal, thus resembling the condition in *Yamaceratops*.

JUGAL: Only the right jugal of the holotype is preserved in its entirety (fig. 1). It appears to be less symmetrical in lateral view than the jugal of other basal neoceratopsians. Rostrally, the jugal tapers to a point that contacts the rim of the antorbital fossa, whereas the caudal end is deeply expanded and lobate in shape. This rostrocaudal asymmetry contrasts with the jugals of taxa such as *Archaeoceratops* (IVPP V11114), *Leptoceratops* (CMN 8887, 8889), *Protoceratops* (AMNH 6466), and *Udanoceratops* (PIN 3907/11), which exhibit a greater symmetry between the depth of the suborbital and subtemporal parts of the jugal. In these taxa, the rostral tip of the jugal is expanded and participates in the rim of the antorbital fossa, while the caudal end tapers to a point below the infratemporal fenestra. The jugal of *Yamaceratops* resembles the jugal of *Liaoceratops* (Xu et al., 2002) more closely than those of other basal neoceratopsians. In *Liaoceratops* the suborbital part of the jugal tapers strongly, whereas the subtemporal part is markedly deep. Unlike *Yamaceratops* and other more derived neoceratopsians, however, the suborbital part of the jugal is truncated and the quadratojugal is visible in lateral view in *Liaoceratops*. An equal or greater depth of the suborbital part of the jugal relative to the temporal ramus has been proposed as a synapomorphy of Ceratopsia by various authors (Sereno, 2000; You and Dodson, 2003), but is not present in *Liaoceratops* and *Yamaceratops*.

The articulation for the maxilla is visible in the partial right jugal of IGM 100/1303 (fig. 6). A narrow groove that rises anteriorly marks the lateral articulation with the maxilla.

This groove is backed by a smooth wall of bone that forms a narrow ridge separating the lateral and medial parts of the maxillary articulation in ventral view. The medial part of the articulation is a broad sulcus that received the posteromedial fingerlike process of the maxilla. Just dorsal to the medial maxillary articulation, the medial face of the jugal exhibits a low pyramidal mound that articulates with the tip of the lateral process of the ectopterygoid (fig. 6).

A narrow but deep notch invades the infratemporal border of the jugal at the base of the dorsal process and reaches almost halfway to the orbital border on the holotype skull (fig. 1). This embayment is surrounded by a smooth-walled depression in the bone, and no similar feature has been reported from other ceratopsian specimens. In several respects, this structure is similar to bone lesions interpreted as pathologies in some dinosaur specimens, including a mature *Psittacosaurus mongoliensis* (IGM 100/1132). However, without at least one more complete jugal, it remains uncertain whether this feature is a phylogenetic character or pathologic in origin.

The dorsal process of the jugal is elongate and contacts the squamosal along the dorsal rim of the infratemporal fenestra and excludes the postorbital from participating in the border of the fenestra (fig. 1). It appears to reach almost as far caudally as the postorbital. In *Protoceratops* (AMNH 6418, 6429, 6466), *Archaeoceratops* (IVPP V11114), and *Leptoceratops* (CMN 8887), the dorsal process of the jugal terminates level with or just rostral to the postorbital.

Caudal to the dorsal process, the subtemporal wing of the jugal flares and has a roughly rhomboid shape. The posterior edge is expanded laterally to form an oblique ridge, in place of the more pointed hornlike structure seen in coronosaurs such as *Protoceratops* and ceratopsids. This ridge is more laterally directed and not as prominent as the epijugal ridge of *Udanoceratops* and other leptoceratopsids, and is most similar to *Archaeoceratops* in its orientation and relative size. The convex caudal face of the ridge is rugose for reception of the epijugal (fig. 3).

The external surface of the jugal is lightly textured and marked by a number of small neurovascular foramina. One of these, located near the base of the dorsal process, appears to pass directly through the jugal, unlike in other ceratopsians with the exception of an unpublished specimen of *Liaoceratops* (P. J. Makovicky, personal obs.).

EPIJUGAL: A well-preserved epijugal (fig. 7) was discovered with the holotype skull and presumably belongs with the complete right jugal. It is an elongate, crescent-shaped bone as in leptoceratopsids (AMNH 5464; CMN 8887, 8889), and would have attached to a long stretch of the caudodorsal edge of the jugal ridge. Its lateral surface is gently convex and is marked by vascular grooves (fig. 7B) that are typical of skull parts that bore a keratinous cover. The medial face is smooth and is concave (fig. 7A). An epijugal is absent in *Liaoceratops* and more basal ceratopsian taxa, but appears to be present in all other neoceratopsians.

LACRIMAL: Only the posterior part of each lacrimal, bearing the antorbital fossa rim and the orbital margin, is preserved on the holotype (figs. 1, 2). The antorbital fossa is deeply excavated on to the lateral surface of the lacrimal, and it presumably formed the caudal border of the antorbital fenestra as in *Protoceratops andrewsi* (Brown and Schlaikjer, 1940b). The lacrimal contacts the maxilla ventrally and the jugal caudally and abuts a transverse ridge of the palatine along the cruciform roof of the palate (fig. 2) as in protoceratopsids (Osmólska, 1986) and ceratopsids (Hatcher et al., 1907).

PREFRONTAL: The prefrontal is L-shaped with a descending ramus that bounds the orbit rostrally, and a posterior process that forms much of the dorsal rim of the orbit (figs. 1, 3). The two rami are perpendicular to each other, and the posterior ramus is the longer of the two. The prefrontal is flat dorsally, and has a gently concave lateral border, but is not sinuous as in the juvenile specimens that were used to diagnose *Protoceratops kozlowskii* (= *Bagaceratops*) (Maryanska and Osmólska, 1975). At the juncture of the ventral and posterior rami, the medial face of the prefrontal is deeply concave.

FRONTAL: The frontals of the holotype specimen are fused along the midline, although the sutural line is still faintly percep-

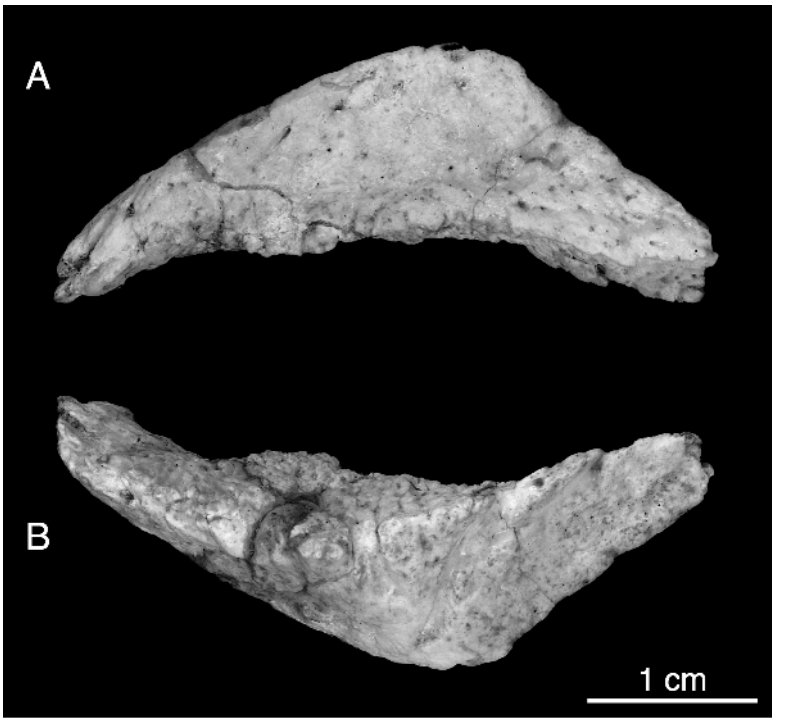

Fig. 7. Right epijugal of the holotype specimen of *Yamaceratops dorngobiensis* (IGM 100/1315), in medial (**A**) and lateral (**B**) views.

tible (fig. 3). At the rostral midline, the frontals form a sharp wedge between the posterior ends of the nasals. Each nasal would have overlapped a striated, sutural surface on the frontal adjacent to the prefrontal. The skull table is slightly concave between the sutures for the postorbitals. The supratemporal fenestra has a gentle emargination on to the posterior edge of the frontal (fig. 3), but it is not incised as markedly as in *Protoceratops andrewsi* (AMNH 6429), *Leptoceratops* (CMN 8889), or *Liaoceratops* (IVPP V12738). The suture with the postorbital is broad and sinuous in dorsal view with a lappet of the postorbital overlapping the frontal rostrally and a lappet of the frontal overlying the postorbital caudally. This sinuous morphology is seen in other basal ceratopsians, including *Psittacosaurus mongoliensis* (AMNH 6254), *Liaoceratops* (IVPP V12738), and *Leptoceratops* (CMN 8889), but appears to be a plesiomorphic character state and is also seen in *Hypsilophodon* (BMNH R2477) and *Lesothosaurus* (BMNH RU B23).

POSTORBITAL: As in other neoceratopsians, the postorbital is a triangular plate of bone that extends from the posterior edge of the orbital margin and onto the temporal bar. Its external surface is slightly rugose, as in other neoceratopsians, suggesting tight adherence between the bone and the overlying skin. Along the orbital rim, the postorbital overlaps the jugal along an oblique suture that extends dorsomedially from the lower part of the orbit to its midheight, above which the postorbital exclusively forms the orbital rim. The posterodorsal corner of the orbit is transversely concave, and bounded laterally by a small convex lip. Dorsally, the upper edge of the postorbital overhangs the supratemporal fenestra as in most neoceratopsians with the exception of the leptoceratopsids *Leptoceratops*, *Montanoceratops* (Makovicky, 2001), and *Prenoceratops*.

The ventral edge of the postorbital is slightly concave overall as in *Liaoceratops* (Xu et al., 2002) and is divided into two gently concave sections separated by a small, shallow

point located just dorsal to the embayment along the front edge of the infratemporal fenestra. Caudally, the postorbital inserts into the bifid rostral end of the squamosal as in *Liaoceratops*, *Archaeoceratops*, and leptoceratopsids.

SQUAMOSAL: Only the incomplete right squamosal is preserved on the holotype specimen (fig. 1). It is missing the caudalmost edge that forms the lateral corner of the frill (fig. 3). The squamosal bears two ventral processes that wrap around the head of the quadrate, a long, bifid rostral process that articulates with the postorbital and a broad, medial lappet that overlaps the parietal within the supratemporal fenestra. The rostral process wraps around the caudal end of the postorbital, such that a longer lateral and a shorter medial exposure are visible between the prongs of the squamosal (fig. 1). The ventral prong contacts the jugal along the rim of the infratemporal fenestra, but the location of the suture is difficult to determine given the large number of cracks along the edge of the temporal bar. We interpret the contact as lying just rostral to the caudalmost point of the postorbital. The rostral process of the squamosal is deeply bifid in the leptoceratopsids *Montanoceratops* (AMNH 5464) and *Leptoceratops* (CMN 8887). The sutural boundaries among the bones forming the temporal bar in *Archaeoceratops* are obscure, but the reconstruction presented by You and Dodson (2003) in which the squamosal has no rostral process is unlike the squamosal of any ornithischian and likely incorrect. *Protoceratops* (AMNH 6466) has a squamosal with a long rostral process that is slightly forked for reception of the postorbital. Ceratopsids have a wide zigzag suture between the postorbital and squamosal.

The medial process of the squamosal is lappet-like, but relatively less expanded than in *Liaoceratops* and psittacosaurs (fig. 3). The more rostral of the two processes bracing the head of the quadrate arises from the ventral edge of the medial process, but because of breakage, its length cannot be determined. The main body of the squamosal at the juncture of the processes forms a gently convex lateral surface (fig. 1) at the caudal end of the temporal bar, which suggests that the dorsal edge of the squamosal curved gently to join the parietal frill as in *Liaoceratops* (CMN 8887, 8889). This observation is bolstered by the shape of the caudolateral corner of the supratemporal fenestra in dorsal view (fig. 3). The squamosal makes a smooth, open transition to the frill margin, unlike the acute, slitlike frill corner in coronosaurs (Sereno, 2000; Makovicky, 2001). The broken laterodorsal edge of the fenestra is relatively robust, suggesting that the frill may have had a thickened edge as in *Liaoceratops*. The ventral edge of the squamosal frill margin is caudally concave in lateral view and gently convex transversely.

PARIETAL: What little is present of the parietal in the holotype skull is poorly preserved (fig. 3). The parietal meets the frontal along a zigzag suture that is oriented transversely and lies just caudal to the rostral emargination of the supratemporal fenestra. It forms the steep-sided medial walls of the supratemporal fenestrae, which are separated by a sagittal crest. The height of the sagittal crest is indeterminate because of breakage. Caudally, the frill portion of the parietal meets the dorsal edge of the paroccipital process along a straight, horizontal suture. The length and shape of the frill cannot be determined, as the entire margin is lost to erosion. Poor preservation also precludes observations on the nature of the contact between the parietal and the elements that constitute the sidewall of the braincase. On the occipital surface of the skull, the dorsal end of the supraoccipital fits into a slot along the ventral edge of the parietal as in other basal neoceratopsians (fig. 8).

QUADRATOJUGAL: As in neoceratopsians more derived than *Liaoceratops*, the quadratojugal is transversely wide and more exposed in occipital view than it is laterally (figs. 1, 8). The quadratojugal is crescent shaped in lateral aspect with a convex caudal surface that follows the curve of the jugal crest and a concave rostral surface that walls off the infratemporal fenestra caudally. In this respect, the quadratojugal appears similar to that of *Montanoceratops* (AMNH 5464), which also appears curved to follow the outline of the jugal horn. Dorsal to the overlap by the jugal, the quadratojugal

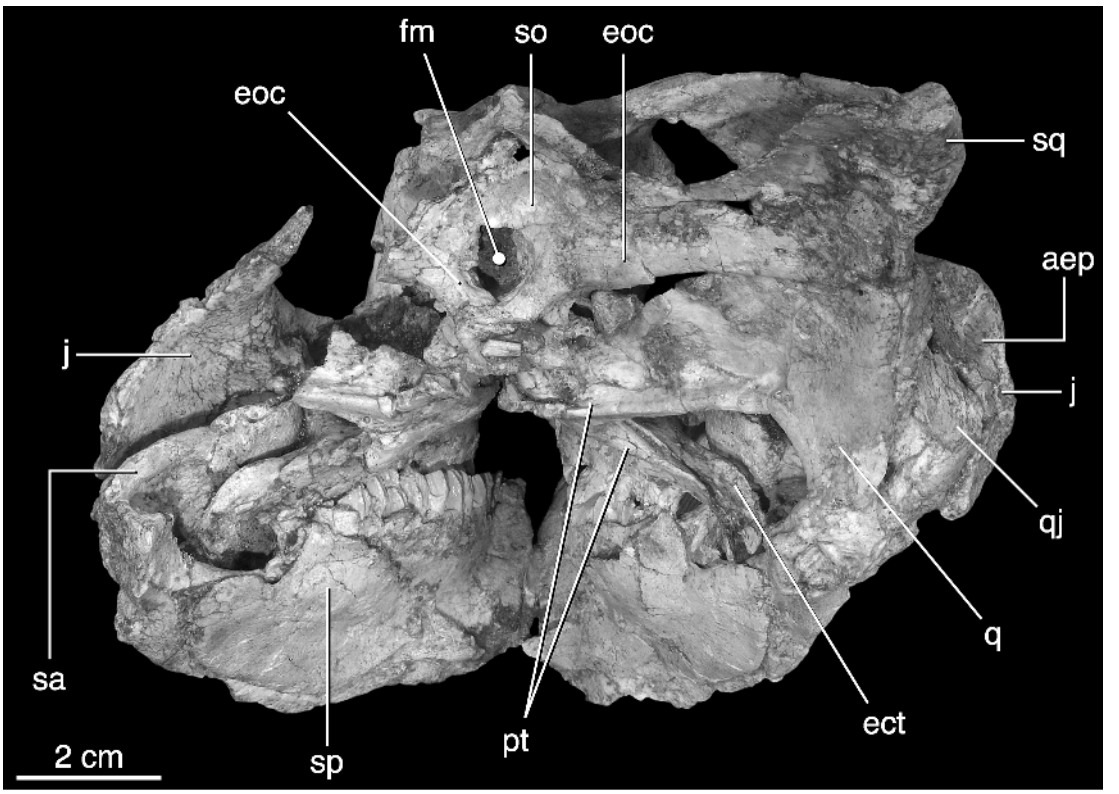

Fig. 8. Occipital view of the holotype skull of *Yamaceratops dorngobiensis* (IGM 100/1315). Abbreviations are listed in appendix 3.

apparently bears a short dorsal spine that adheres to the lateral edge of the quadrate. This process is mostly missing in the holotype, but its length can be deduced from the corresponding contact on the quadrate. A similar overlap of the quadrate by a pointed dorsal process of the quadratojugal is observed in *Liaoceratops* (IVPP V12738).

QUADRATE: The quadrate has a nearly straight, rostrocaudally compressed shaft as in other neoceratopsians (figs. 1, 9). The quadrate head is tall and narrow and flanked caudally by a straight ridge that marks the contact with the caudoventral process of the squamosal and the tip of the paroccipital process. A broad, triangular pterygoid wing extends from the medial edge of the shaft for most of its length and terminates at the quadrate head (fig. 9). The distal condyles are asymmetric and separated by a shallow groove into a larger lateral and smaller medial articulation, unlike the flat condylar articulation of psittacosaurids. A sinuous ridge runs along the lateral face of the quadrate shaft marking the caudal edge of the sutural surface for the quadratojugal. It extends from the lateral condyle up the caudal edge of the shaft, curves rostrally at the midheight of the shaft, and terminates along its rostral edge about one-third of the way down from the quadrate head. A similar extensive ridge is present along most of the lateral surface of the quadrate shaft in *Liaoceratops*, but the extent of this ridge becomes relatively shorter in more derived taxa, such as *Protoceratops*, in which it only reaches about halfway up the quadrate shaft. As in the basal ceratopsian *Chaoyangsaurus*, the lateral edge of the shaft bears a short rostral process that underlaps the quadratojugal (fig. 9). Its length is indeterminate due to breakage, but it is unlikely that it reached the jugal. This plesiomorphic feature

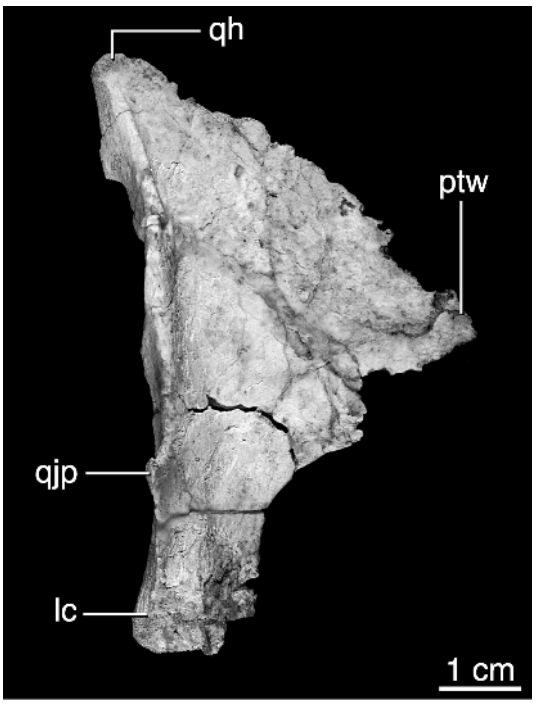

Fig. 9. Right quadrate of the referred specimen of *Yamaceratops dorngobiensis* (IGM 100/1303) in oblique rostrolateral view. Abbreviations are listed in appendix 3.

has not been reported in more derived ceratopsians, and is apparently also absent in *Psittacosaurus mongoliensis* (IGM 100/1032).

BRAINCASE: Erosion has obscured many braincase features, including many of the sutural contacts. The laterosphenoids form the rostrolateral walls of the braincase dorsal to the hypophysial fossa. They meet at the midline to separate the optic nerve exits from the olfactory nerve tract. Each laterosphenoid bears a prominent capitate process that reaches laterally to underlap the postorbital–frontal contact. A small foramen for exit of the trochlear nerve (CN IV) pierces the wall of the laterosphenoid dorsally, just rostral to the base of the capitate process. The sutures between the laterosphenoid and prootic or the prootic and opisthotic cannot be made out. A long external auditory meatus extends laterally from the middle ear as a groove along the ventral edge of the paroccipital process as in other neoceratopsians (fig. 10). A triangular slip of the supraoccipital is exposed inside the supratemporal fenestra along the base of the paroccipital process and wedges between the exoccipital and the parietal (fig. 3).

The supraoccipital is formed as a low, wide triangle and participates in the margin of the foramen magnum (fig. 10). A low, vertical midline ridge extends from the edge of the foramen magnum to the contact with the parietal. A midline ridge is variously developed among some basal neoceratopsian taxa including *Leptoceratops*, *Protoceratops*, and *Montanoceratops*, where it is split by a drop-shaped depression ventrally (Makovicky, 2001).

The condylar region of the holotype specimen is poorly preserved, but the exoccipitals appear to meet along the floor of the medullar region (fig. 8). This suggests that they formed the dorsal part of the occipital condyle, and the basioccipital did not join in flooring the medulla oblongata. The basioccipital flares laterally below the condyle, to form the large basioccipital tubera characteristic of ceratopsians (Makovicky, 2001). A shallow but wide notch separates the tubera at the ventral midline and forms the caudal border of a small pit between the basioccipital and basisphenoid (fig. 10). Such a pit is also observed in some but not all specimens of *Protoceratops* and *Bagaceratops* and was identified as a median Eustachian system as in crocodilians (Maryanska and Osmólska, 1975). It does not connect to the middle ear region, however, and its variable intraspecific occurrence within several neoceratopsian species argues against such a homology (Makovicky, 2001).

The basipterygoid processes are relatively robust and short as in *Liaoceratops* and unlike the more elongate and slender processes of *Protoceratops* or the recurved ones that are diagnostic of leptoceratopsids (Chinnery and Weishampel, 1998; Makovicky, 2001). They project lateroventrally below the hypophysial fossa as in other neoceratopsians, but unlike psittacosaurids and other outgroups, in which they are directed rostrolaterally. A triangular, bladelike cultriform process projects rostrally from between the basipterygoid processes.

PALATINE: The palatines are inclined to form the posterior part of the highly vaulted palate (figs. 2, 10). Each palatine is a large subtriangular plate that overlaps the medial

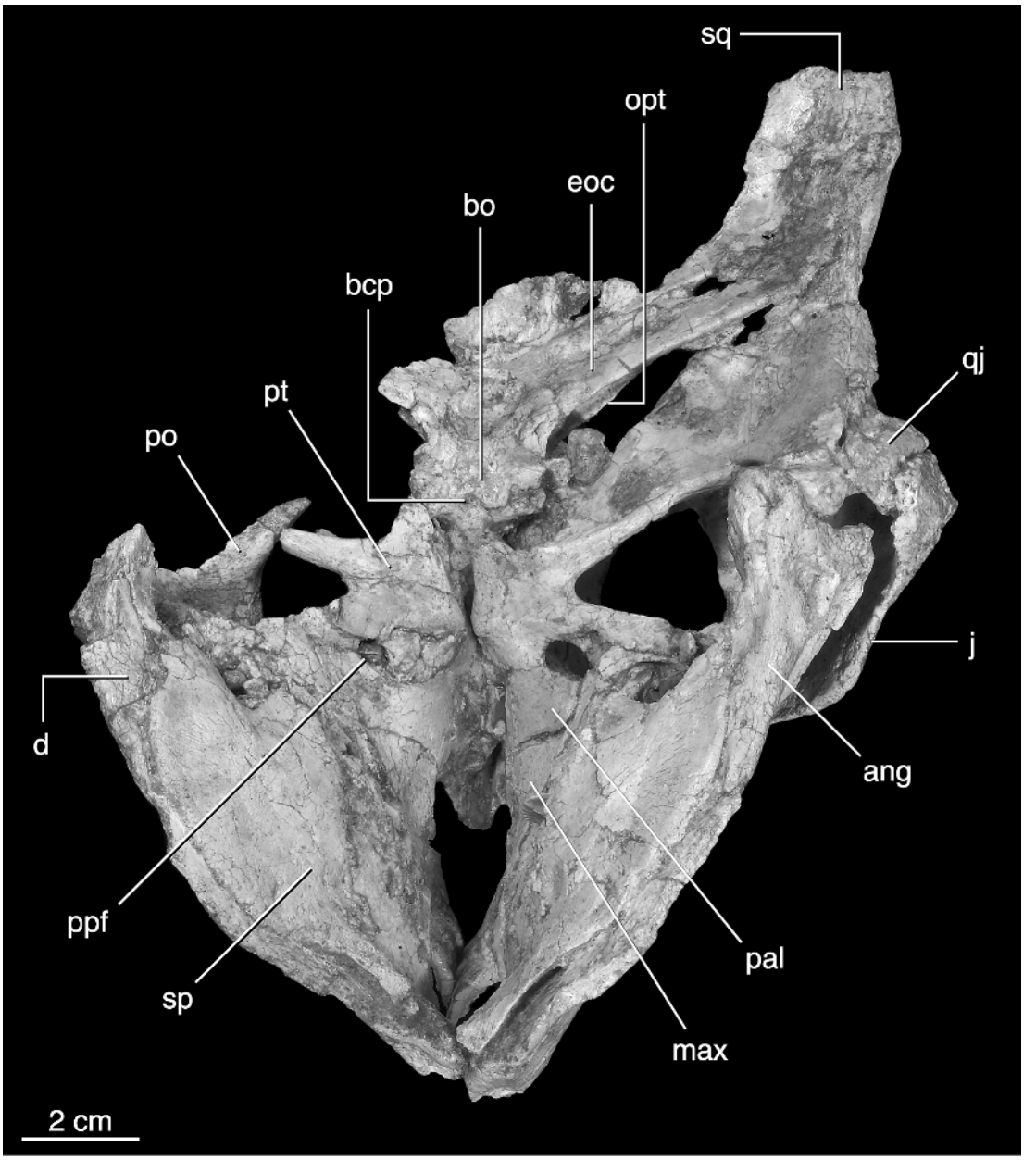

Fig. 10. Ventral view of the holotype skull of *Yamaceratops dorngobiensis* (IGM 100/1315). Abbreviations are listed in appendix 3.

surface of the maxilla along an oblique suture extending from the caudal end of the choana to the ectopterygoid as in *Protoceratops* (PIN 614/7; Osmólska, 1986). Medially, the palatines meet to form the base of the interchoanal septum, which is broken in the holotype (fig. 2). The missing vomers presumably slotted into the narrow roof of the palate in this region. Caudal to the choana, the dorsal surface of the palatine bears a transverse lamina that abuts the lacrimal laterally. The transverse laminae of both palatines meet the

sharp apex of the palatal roof in a cruciform juncture that is a derived character of many neoceratopsians (Osmólska, 1986). Along its caudomedial edge, each palatine forms the rostral rim of the pterygo-palatine foramen (Brown and Schlaikjer, 1940b), which is a reduced homolog of the sauropsid suborbital fenestra. The pterygo-palatine fenestra (figs. 10, 11) is proportionately quite large in *Yamaceratops* as in *Liaoceratops*, *Psittacosaurus*, and *Chaoyangsaurus*, unlike the relatively diminutive foramen observed in coronosaurs.

PTERYGOID: The pterygoid is a complex tetraradiate bone that contacts the palatine, ectopterygoid, basipterygoid, and quadrate, as well as the other pterygoid along the midline (fig. 10). The four rami converge on the main moiety of the pterygoid, which forms the caudal end of the palate just ventral to the braincase. A narrow gap separates the palatal bodies of the pterygoids, but it is unclear how much of this may be due to postmortem distortion of the skull. Such a gap is also observed in *Prenoceratops* (B. Chinnery-Allgeier, personal commun.). Each rostral process is triangular, inclined rostrodorsally, and meets its counterpart at the midline. Together, the triangular rostral processes slot into the vaulted palatal roof formed by the palatines, which partly overlap the rostral pterygoid processes laterally. A small gap between the tips of the pterygoids and the apex of the vault formed by the palatines presumably held the caudal ends of the vomers.

Just caudal to the pterygoid rim of the pterygopalatine fenestra, a long, slender mandibular process projects lateroventrally from the lateral edge of the pterygoid. It extends along the caudal rim of the palate and projects beyond the caudal end of the tooth row. The mandibular process underlaps the ventral process of the ectopterygoid along its full length, and together they form the palatal mandibular process that channels M. pterygoideus towards its insertion on the mandible (Galton, 1974).

The strongly flared quadrate wing of the pterygoid rises abruptly from the caudal part of the palatal body. At its base, the quadrate wing forms the narrow pocket for articulation with the basipterygoid processes. It flares widely at its distal end to overlap the pterygoid wing of the quadrate. An elongate, slitlike opening extends between the dorsal edge of the quadrate wing of the pterygoid and the base of the paroccipital process. A short caudal process projects along the midline, caudal to the facet for reception of the basipterygoid process as in other basal ceratopsians (fig. 10). It appears to be pointed rather than lobate as in *Liaoceratops* (IVPP V12738).

ECTOPTERYGOID: The ectopterygoid is widely exposed on the palate in contrast to the condition in more derived neoceratopsians (fig. 11). It is triradiate with a wide but short lobe that extends on to the pterygoid, a strongly curved lobe that abuts the jugal, and a long ventrally curved process that is sutured to the pterygoid to form the ventral process that channeled the M. pterygoideus dorsalis (figs. 3, 11). In *Yamaceratops*, as in *Chaoyangsaurus* (IGCAGS V371) and *Liaoceratops* (IVPP V12738), a ventral trough excavates the base of the ectopterygoid for reception of the caudal end of the maxilla. The ectopterygoid thus separates the maxilla and pterygoid as in *Liaoceratops* and outgroup taxa such as *Hypsilophodon* (Galton, 1974; BMNH R2477). In more derived taxa, especially in ceratopsids, the ectopterygoid is reduced and the pterygoid contacts the caudal edge of the maxilla (Brown and Schlaikjer, 1940b).

In its robustness and participation in formation of the ventral process, the ectopterygoid is similar to those of *Chaoyangsaurus* (IGCAGS V371), *Liaoceratops* (IVPP V12738), and *Leptoceratops* (Sternberg, 1951) and juvenile *Protoceratops* (Brown and Schlaikjer, 1940b). In adult *Protoceratops*, the ectopterygoid has a very reduced exposure on the roof of the palate (Brown and Schlaikjer, 1940b; AMNH 6466), and this element is entirely excluded from palatal view in ceratopsids (Hatcher et al., 1907; Brown and Schlaikjer, 1940b). In *Yamaceratops* (fig. 11), as in *Liaoceratops*, *Leptoceratops* (Sternberg, 1951), and *Protoceratops* (Brown and Schlaikjer, 1940b), the ectopterygoid participates in the border of the pterygopalatine fenestra, as is primitive among dinosaurs. The pterygopalatine is much reduced in adult

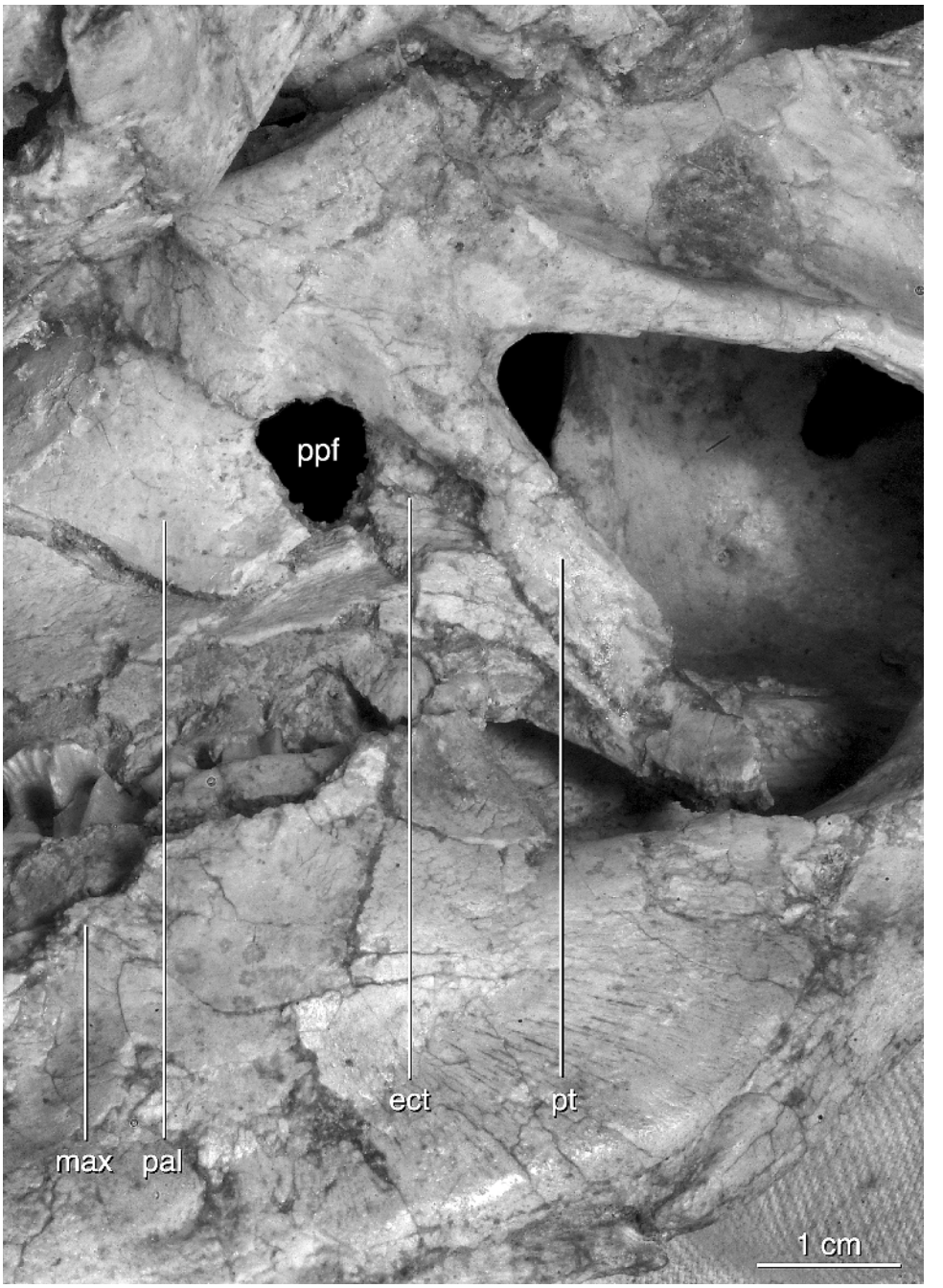

Fig. 11. Oblique close-up of the right caudal region of the palate of the holotype skull of *Yamaceratops dorngobiensis* (IGM 100/1315). Abbreviations are listed in appendix 3.

Protoceratops and ceratopsids relative to more basal forms, and an ectopterygoid contribution to the border of this opening is entirely lost in ceratopsids.

PREDENTARY: Neither the holotype nor the referred partial specimen preserves the predentary, but an isolated partial basal neoceratopsian predentary (IGM 100/1867) was collected at the Kughenetslavkant locality and is referred to *Yamaceratops* (fig. 12). The element is missing most of its caudal end, including the labial and ventral processes. In dorsal view, the rostral end forms an acute point. The predentary is relatively solid and the buccal surface is only slightly concave as in the basal taxa *Chaoyangsaurus*, *Liaoceratops*, and *Archaeoceratops* in contrast to the scoop-shaped predentary of *Leptoceratops*, *Protoceratops*, and ceratopsids. The tip is slightly recurved in profile (fig. 12) and would probably have curved dorsally in life. As in most other basal neoceratopsians, the edges of the predentary are beveled and not sharp or grooved as in ceratopsids.

DENTARY: The dentary has a gently curved ventral edge, but does not bear an everted flange as in *Liaoceratops* and some psittacosaurid species (fig. 1). Each dentary bears a prominent lateral ridge that extends from the base of the coronoid process to the symphysis, and the tooth row is deeply inset from the buccal margin. The mandibular symphysis is broad and faces anteriorly (fig. 2). On the better preserved left dentary of the holotype, a small groove is visible at the rostrodorsal tip of the dentary for reception of the buccal process of the predentary, but unlike in leptoceratopsids, there is no large pit in this region. As in other basal ceratopsians, there is little separation between the articular surface for the predentary and the first tooth position, in contrast to ceratopsids in which a distinct diastema occurs at the tips of the dentary. The coronoid process is well developed and separated from the tooth row by a wide sulcus unlike *Chaoyangsaurus*, *Psittacosaurus*, and *Liaoceratops*. The tooth row terminates level with and medial to the base of the coronoid process (figs. 1, 2) as in higher neoceratopsians.

SPLENIAL: Both splenials are preserved in the holotype (fig. 10). As in other ceratop-

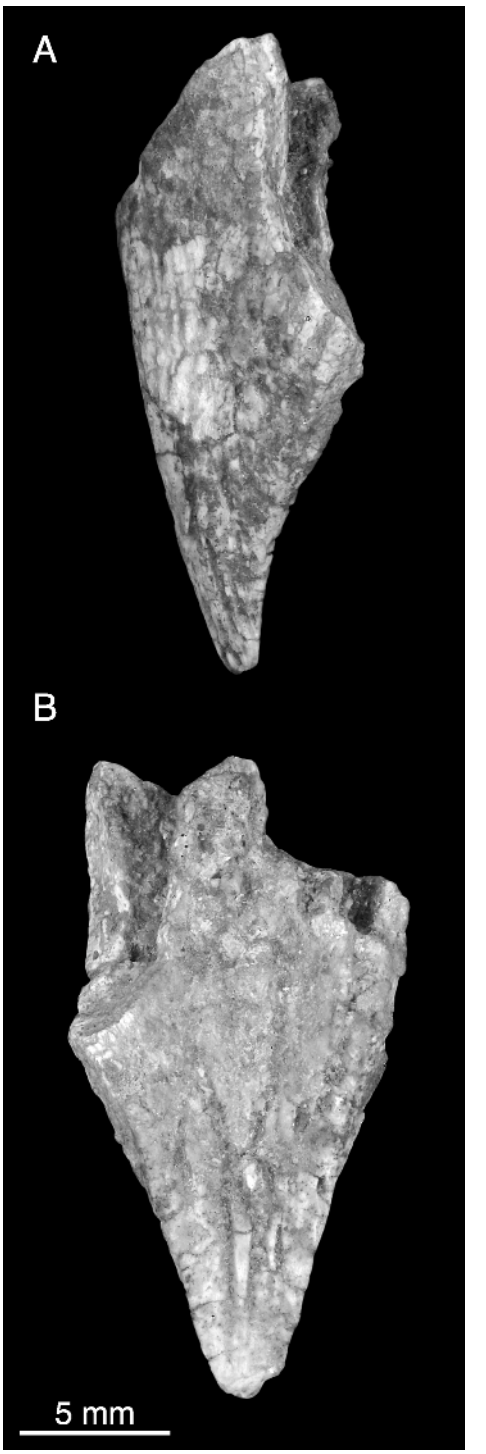

Fig. 12. Isolated predentary (IGM 100/1867) referred to *Yamaceratops dorngobiensis* in lateral (**A**) and dorsal (**B**) views.

sians, the moiety of the splenial is a deeply expanded sheet of bone that overlaps the lingual face of the dentary (figs. 10, 11). The ventral margin of the splenial parallels the ventral edge of the dentary, but the dorsal margin slopes toward the symphysis so that the main body of the bone attenuates rostrally. The rostral end broadens transversely to form a symphyseal process that projects forward to meet its counterpart at the symphyseal midline.

CORONOID: Both coronoids are preserved in the holotype specimen. As in other neoceratopsians, the coronoid consists of an expanded lobe that forms the medial face of the coronoid process and a slender ventral process that curves around the rostrodorsal corner of the adductor fossa. The ventral process is relatively more robust than in *Protoceratops*. A separate intercoronoid is not discernible, but is known to occur in some other neoceratopsians, including *Protoceratops*, some ceratopsids (Brown and Schlaikjer, 1940b), and the basal taxon *Liaoceratops* (P.J. Makovicky, personal obs.).

SURANGULAR: Both surangulars are preserved on the holotype skull, although the left one is missing the glenoid. A disarticulated, but well-preserved, left surangular was found with the referred specimen (fig. 13). The surangular is subtriangular in lateral view (fig. 13A) with the coronoid process forming the dorsal apex. Rostral to the coronoid process, the surangular bears a long, pointed rostral process, which slots into the caudal end of the dentary coronoid process. The lateral surface of this process is striated for sutural contact with the dentary, and grooves extend along the medial and lateral faces of the process adjacent to its dorsal edge. The rostral edge of the coronoid prominence is sharply keeled where it slots between the medial edge of the dentary and the expanded lobe of the coronoid. The caudal edge of the prominence is thickened and rounded and is caudally confluent with a convex wall of bone that delimits the lateral edge of the glenoid (fig. 13D). This lateral glenoid wall is observed in all neoceratopsians with the exception of *Liaoceratops*.

A robust lateral ridge extends along the labial face of the surangular (fig. 13A) as in *Liaoceratops*, *Archaeoceratops*, protoceratopsids, and *Montanoceratops* (Chinnery and Weishampel, 1998). Ventral to the caudal end of the edge and the glenoid, the lateral face of the surangular is depressed to receive the dorsal edge of the angular (fig. 13C). The surangular forms most of the lateral cotyle of the glenoid, which occupies the space between the lateral wall and articulation with the articular. The surangular bears a thin sheetlike medial process that wraps around the rostral end of the articular (fig. 13B). A thin crest that lies medial to the articulation for the angular forms a long, almost flat surface for articulation with the body of the articular (fig. 13A,C). This crest adheres to the full length of the articular and participates in the retroarticular process. The medial face of the coronoid prominence is concave, and a small vascular foramen is present anterior to the medial wing of the surangular, as in other neoceratopsians.

ARTICULAR: The articular is an oblong bone, triangular in cross section with an elliptical articular surface forming the glenoid dorsally and robust ridge forming the ventral edge of the bone (fig. 14). Rostral to the glenoid, the articular bears a short, blunt process that fits against the concave face of the surangular medial process (fig. 14B,C). The elevated glenoid surface is elliptical and gently concave dorsally. Its lateral edge is raised and forms the low but wide ridge that divides the glenoid into medial and lateral cotyla. The articular surface of the glenoid is rugose, and a sinuous line separates it from a small, cup-shaped fossa that lies at the caudal end of the articular dorsal to the retroarticular process (fig. 14B). The fossa, and a small mediodorsal tuber that lies adjacent to it, probably mark the insertion of the mandibular abductors as in crocodilians (Schumacher, 1973). A small foramen pierces the base of the tuber adjacent to its rugose apex, as in *Xuanhuaceratops* (Zhao et al., in press). It may connect to a small foramen and groove on the medial face of the bone (fig. 14A), and could be the trace of the Meckelian chord or, less likely, a foramen aerosum. The tuber is continuous ventrally with the blunt retroarticular process of the articular (fig. 14A).

ANGULAR: Only the right angular of the holotype is nearly complete (fig. 1), as the left

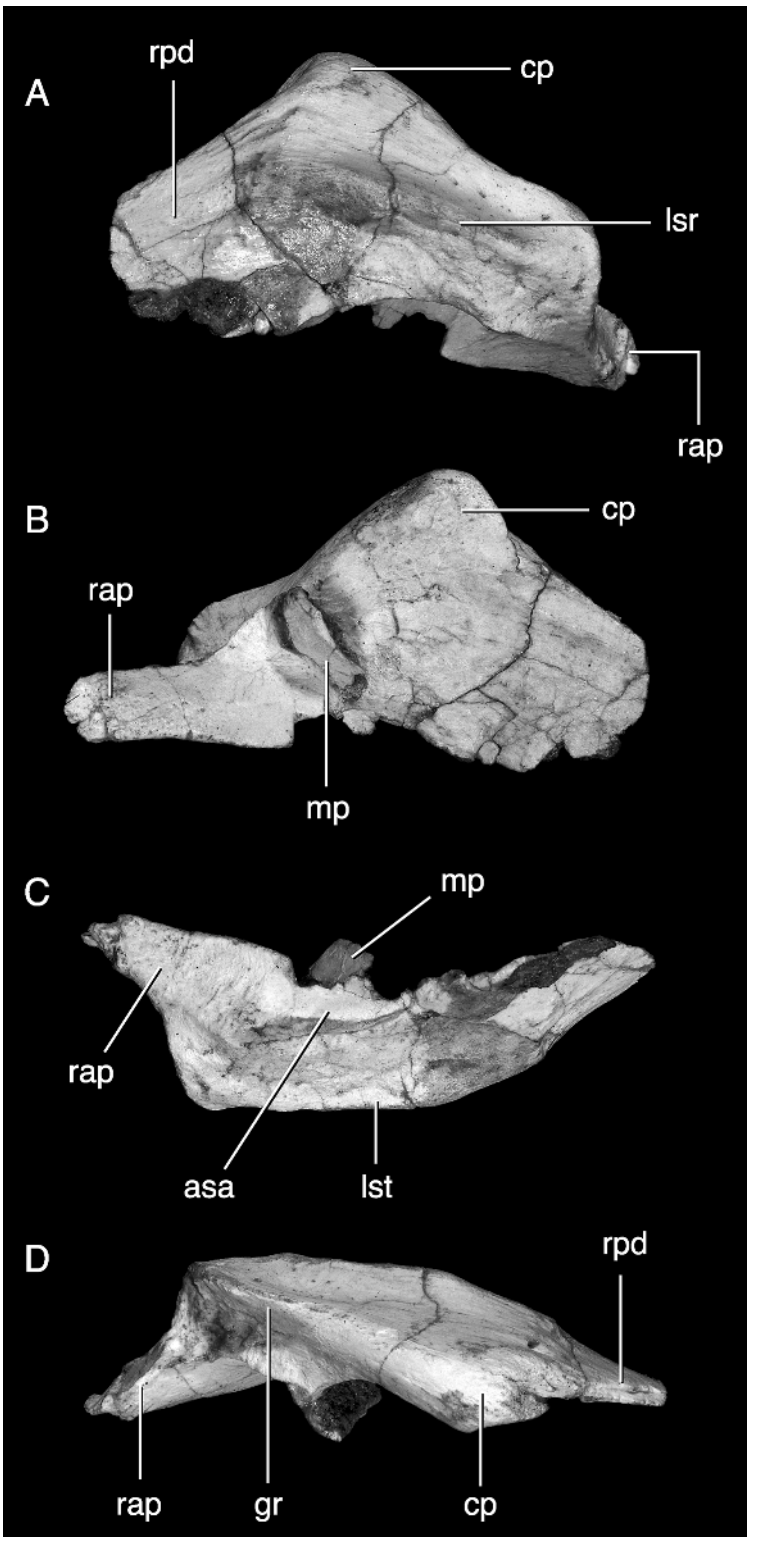

one is missing the caudal end. The angular forms the caudoventral edge of the mandible and overlaps the dentary rostrally and the surangular dorsally. Rostrally, a process of the angular overlaps the caudal end of the dentary near its ventral edge on the lateral face of the jaw (fig. 1). A lappet of the angular also overlaps the ventral edge of the dentary in *Liaoceratops* (IVPP V12633). This lappet is more dorsally placed in *Archaeoceratops* (IVPP V11114), and a narrow, more fingerlike process of the angular slots into the caudal edge of the dentary in *Leptoceratops* (CMN 8889) well above the ventral edge. The contact between the angular and dentary differs in *Chaoyangsaurus* (IGCAGS V371) and *Psittacosaurus*, in which the dentary appears to overlap the angular along the ventral edge of the jaw.

The angular does not bear an everted ridge along its caudoventral edge as in *Leptoceratops* (CMN 8889) and *Protoceratops* (AMNH 6466). Two small bony tubercles are present near the caudal end of the angular, one adjacent to the suture with the surangular and the other, larger one along the ventral margin. In *Liaoceratops* three tubercles are present, but are all linearly arranged along the ventral margin of the bone (Xu et al., 2002). At its caudal end, the angular is deflected medially and embraces the articular from below.

DENTITION: Neither specimen preserves the premaxillary bones, but a single premaxillary tooth appears to be preserved with the referred specimen (fig. 15C). The tooth resembles the premaxillary teeth of *Liaoceratops* in having rostral and caudal carinae, unlike the more cylindrical premaxillary tooth crowns of more derived taxa such as *Protoceratops* (Sereno, 2000). Minute, irregular serrations are present along the basal, unworn section of each carina. Minute serrations are also present on the distal carina of one of the premaxillary teeth in the holotype of *Liaoceratops* (P.J. Makovicky, personal obs.). Both sides of the crown bear a thin layer of enamel. The labial face of the tooth is highly convex, but the lingual side is less convex and bears a small wear facet distally. The root is columnar and almost as wide as the crown. Features that identify this tooth as a premaxillary tooth include the presence of enamel on both crown faces, the near-absence of denticles, lack of a primary ridge, and absence of notch at the distal crown base where the following tooth crown would fit. All "cheek" teeth possess a distinct primary ridge in the holotype specimen of *Yamaceratops*. The unexpected presence of a small wear facet on the lingual face indicates occlusion with the horny rhamphotheca of the predentary.

The maxillary teeth increase in size caudally along the tooth row, with the anteriormost crown being only about half as tall as the crowns near the caudal end of the tooth row. All maxillary crowns are asymmetric around the primary ridge, with the mesial part wider than the distal part. Secondary ridges mark the labial crown faces and terminate in small denticles along the unworn crown tips (fig. 15B). There are five or six denticles along the mesial side of the crown and three along the distal face on the unworn maxillary teeth near the middle of the left tooth row of the holotype. The primary ridges are low and rounded in the smaller, rostral tooth positions, but become better defined on the larger more posterior teeth.

With the exception of the rostralmost tooth, all maxillary teeth have ovoid crowns with mesial and distal edges that are subparallel for much of the crown height. A shallow, mesial groove extends from the tooth onto the base of the crown between the labial and lingual crown faces. It accommodates the rounded distal edge of the root of the preceding tooth. The teeth are closely packed as in other neoceratopsians (Sereno, 2000) and appear to erupt in two, highly coordinated series of *Zahnreihen* (Edmund, 1960). The roots are elliptical in cross section and wider transversely than mesiodistally. In contrast to the premaxillary tooth, all maxillary teeth have

←

Fig. 13. Left surangular of the referred specimen of *Yamaceratops dorngobiensis* (IGM 100/1303) in lateral (**A**), medial (**B**), ventral (**C**), and dorsal (**D**) views. Abbreviations are listed in appendix 3.

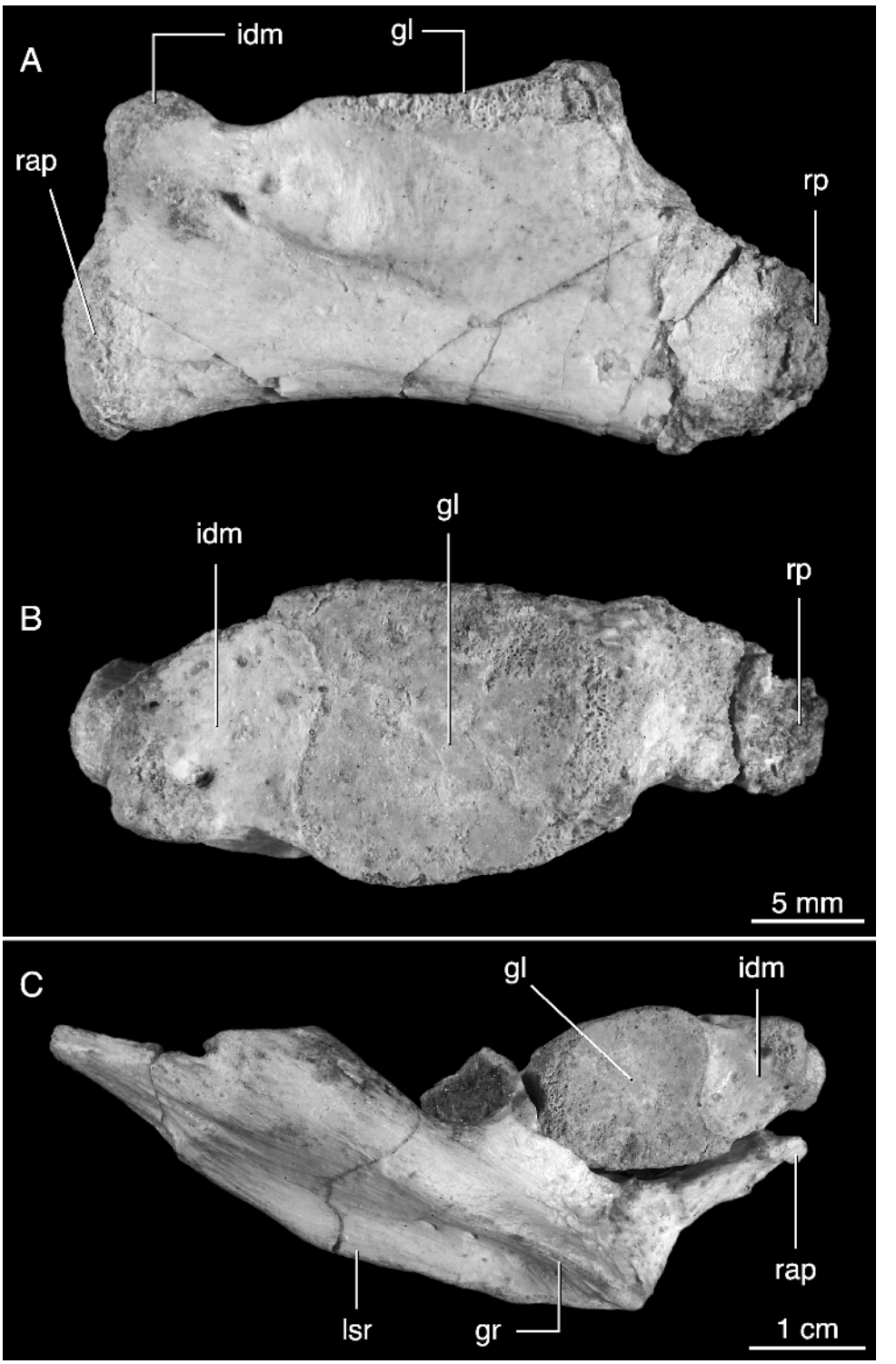

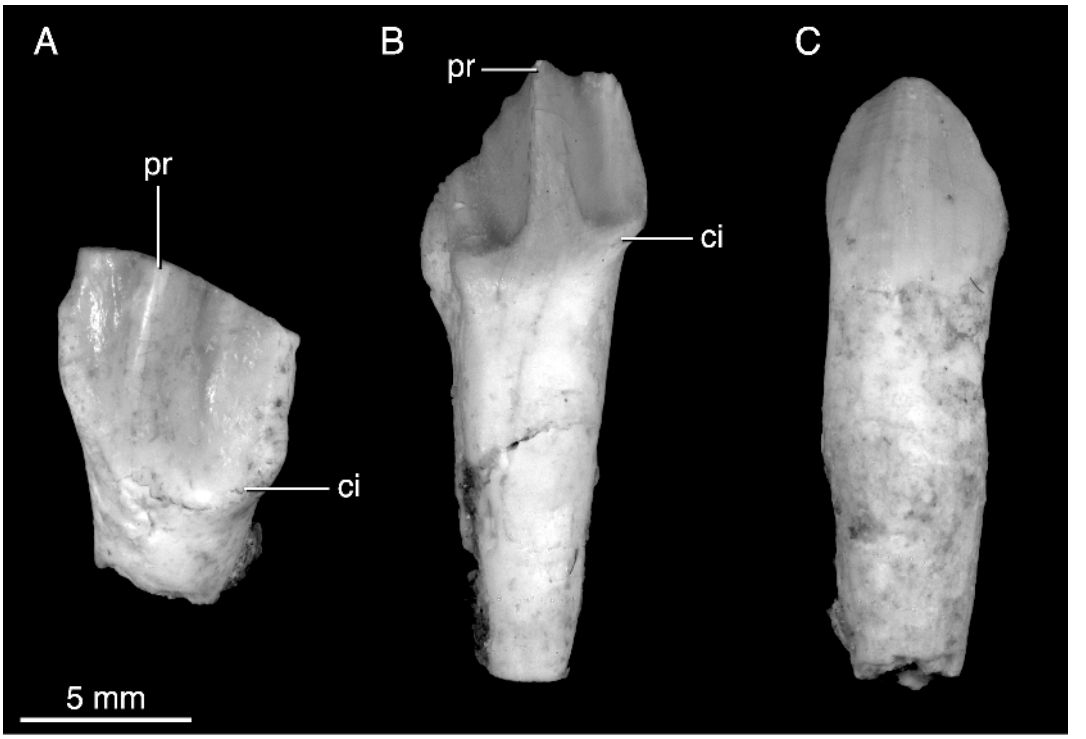

Fig. 15. Isolated teeth from the referred specimen of *Yamaceratops dorngobiensis* (IGM 100/1303). **A**: Larger cheek tooth in nonocclusal view. **B**: Probable anterior maxillary tooth in labial view. **C**: Premaxillary tooth in labial view. Abbreviations are listed in appendix 3.

crowns that are distinctly wider than their respective roots (fig. 15). Although many crowns are either obscured by occlusion with the lower jaw or suffer from poor preservation, all appear to have single wear facets, angled at about 30° to the vertical axis of the tooth. All maxillary and dentary teeth have enamel restricted to the nonocclusal crown faces.

The dentary teeth resemble the maxillary ones, but are proportionately wider and more rounded in lingual aspect (fig. 16). A crestlike primary ridge is present on all dentary teeth, and it subdivides the lingual crown face into a smaller mesial and larger distal parts. Distal secondary ridges are parallel with the primary ridge, but the mesial ones are oriented obliquely to the primary ridge. The number of denticles is 4–5 on the distal edge and 3–4 on the mesial one.

VERTEBRAE: One cervical vertebra, an isolated centrum, and a midcaudal neural arch are the only vertebral elements preserved with the referred specimen. The cervical centrum is poorly preserved, but the neural arch is in better shape, and reveals a short, erect neural spine and highly angled zygapophyseal articular facets. The prezygapophyses only project for a very short distance rostral to the spine, and do not extend beyond the anterior intercentral articulation. The neural canal is very wide. Comparison with vertebral column

←

Fig. 14. Left articular of the referred specimen of *Yamaceratops dorngobiensis* (IGM 100/1303) in medial (**A**) and dorsal (**B**) views and in articulation with left surangular (**C**). Abbreviations are listed in appendix 3.

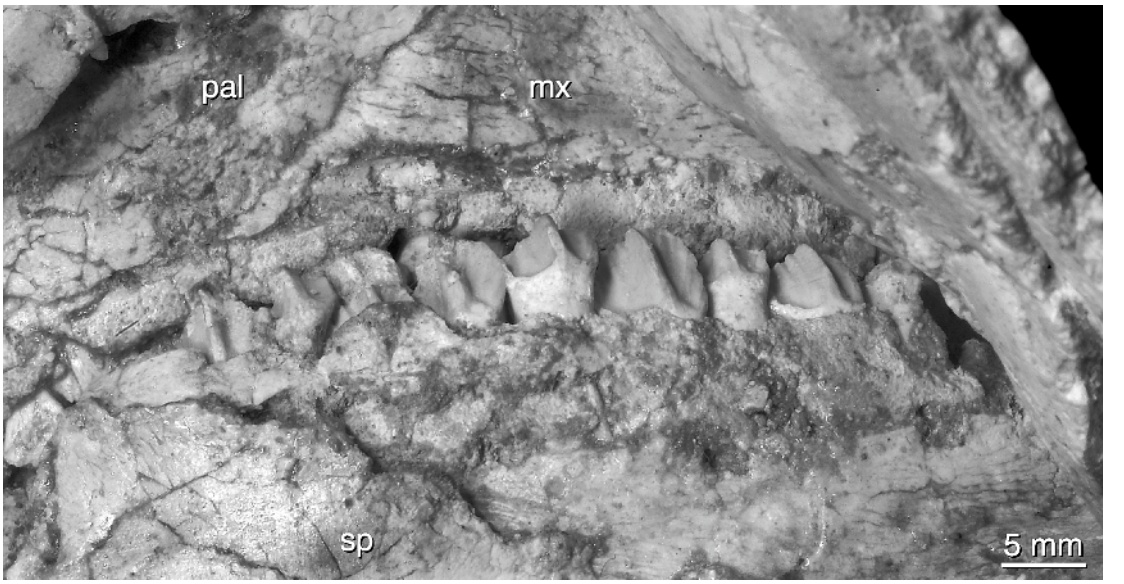

Fig. 16. Left dentary tooth row of the holotype specimen of *Yamaceratops dorngobiensis* (IGM 100/1315). Abbreviations are listed in appendix 3.

of *Protoceratops* suggests that these anatomical features are found near the front end of the cervical series in the third and fourth cervicals. In neoceratopsians the third cervical fuses to the axis to form part of the syncervical early in ontogeny, which suggests that the present element is the fourth cervical.

The isolated centrum has an open suture for contact with the arch, indicative of immaturity (Brochu, 1996). The centrum lacks a chevron facet indicating that it is not a caudal. There is no sign of a parapophysis, which suggests it may be a trunk vertebra in which the parapophyses are situated on the arch.

The isolated midcaudal neural arch (fig. 17) is typical of basal Neoceratopsia in having an elongate and erect neural spine, the tip of which is lost. The closely spaced zygapophyses have near-vertical articular facets and are close together, and the neural canal is narrow.

Pelvic and Hindlimb Elements: A partial left ilium (fig. 18) was associated with the skull bones of the referred specimen of *Yamaceratops*. It preserves the pubic and ischial peduncles as well as the postacetabular blade, but the narrow preacetabular blade has been lost. The pubic peduncle is slender and directed anteroventrally, whereas the ischiadic peduncle is robust and bears a large convex antitrochanter. Unlike in *Archaeoceratops*, the pubic peduncle has a more rounded lateral edge, and the antitrochanter is not excavated by a fossa (You and Dodson, 2003). The iliac blade is low and vertical above the acetabulum. It tapers very slightly toward the distal end, which is crushed, but appears rounded as in other ceratopsians. On its medial face (fig. 18B) impressions for the sacral ribs and transverse processes of sacrals 2–5 are visible and resemble the pattern in other basal neoceratopsians.

A distal end of a right femur was recovered with the referred specimen. It does not differ markedly from the femur of other basal ceratopsians. A pedal phalanx and an ungual (fig. 19) were also recovered. The phalanx is longer than wide and broader than tall in proximal view with a transversely convex articular surface. The distal articular surface is marked by wide, shallow ginglymus. The ungual is missing the tip, but would have terminated in a pointed claw rather than a rounded hoof. It is only slightly curved in lateral view, and has deeply incised claw sheath grooves (fig. 19A).

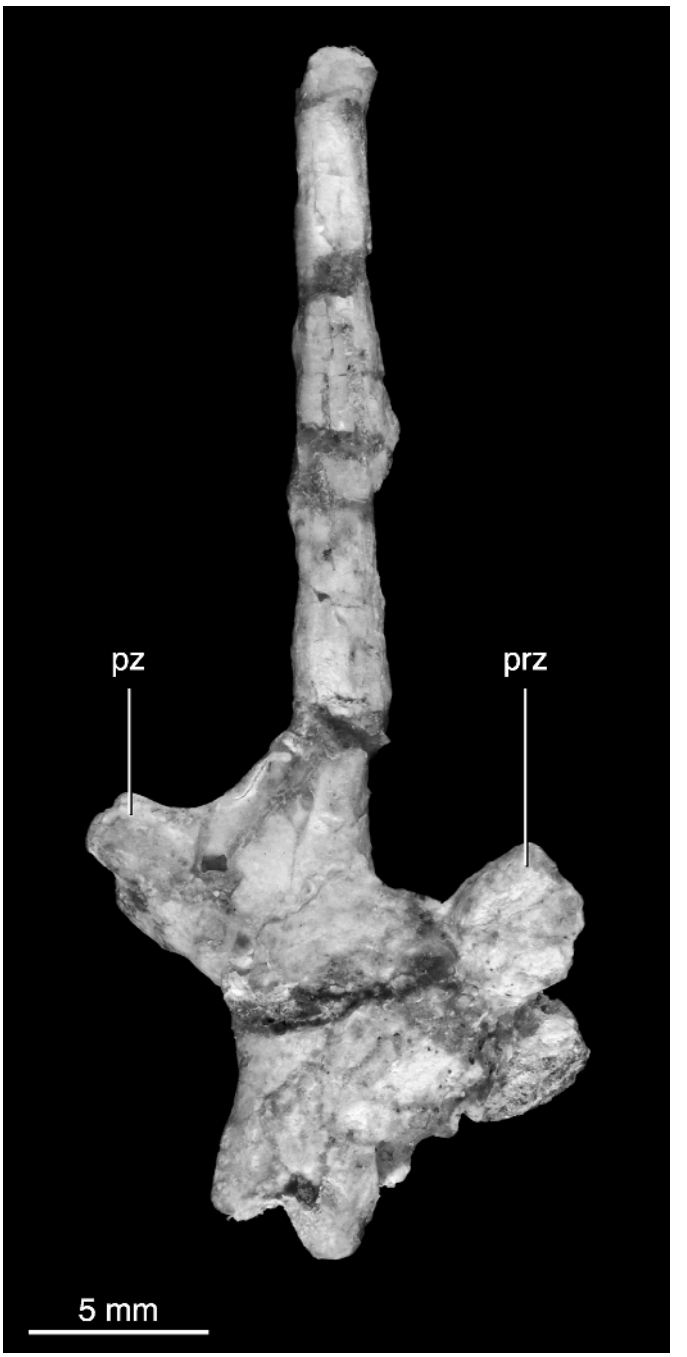

Fig. 17. Caudal neural arch of the referred specimen of *Yamaceratops dorngobiensis* IGM 100/1303) in lateral view. Abbreviations are listed in appendix 3.

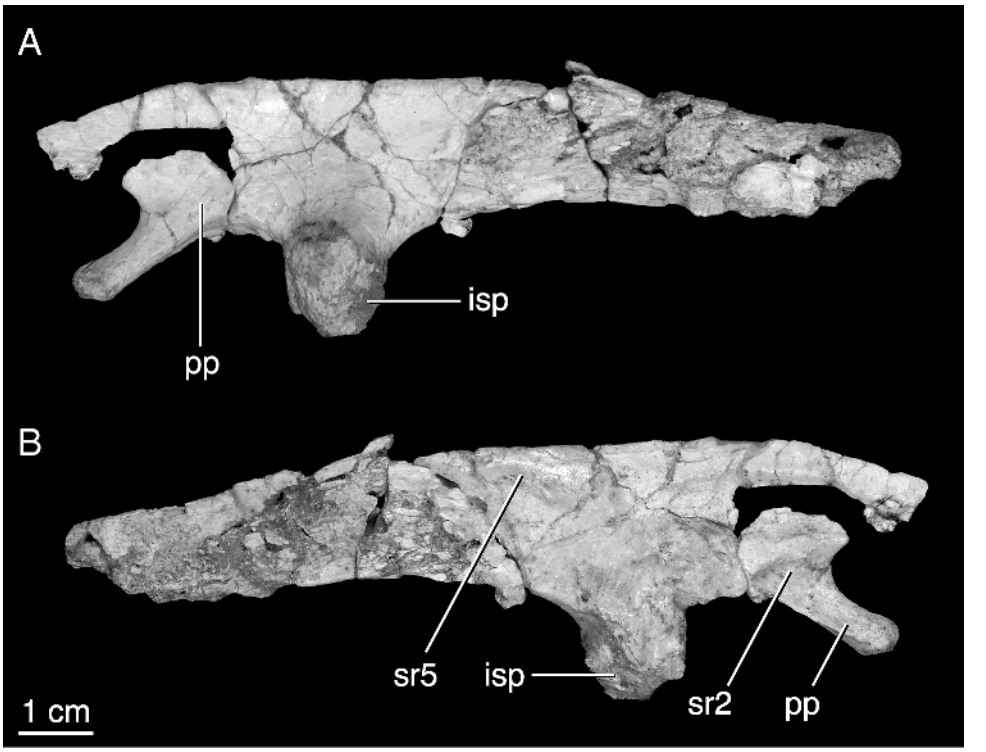

Fig. 18. Left ilium of the referred specimen of *Yamaceratops dorngobiensis* (IGM 100/1303) in lateral (**A**) and medial (**B**) views. Abbreviations are listed in appendix 3.

PHYLOGENETIC ANALYSIS

Yamaceratops gobiensis represents a new basal neoceratopsian taxon. To determine its phylogenetic position, we added it to a revised version of the cladistic matrix developed in Xu et al. (2002). A number of revisions and changes were made to the matrix, including the addition of 13 new characters and recoding of several observations based on restudy of the relevant specimens. Details regarding character and taxon sampling are discussed in the following two sections. Since the publication of the Xu et al. (2002) study, several new taxa have appeared in print and remarks on these are also presented below.

TAXONOMIC SAMPLING: The matrix comprises 20 putatively valid taxa at generic level, except for two species of *Psittacosaurus*. The validity of all but two of these taxa was recently reviewed and supported by autapomorphies (Makovicky, 2002). The two taxa *Asiaceratops* and *Graciliceratops* are of more questionable status. *Asiaceratops salsopaludalis* was erected for an assemblage of isolated elements from the Cenomanian Khodzhakul Svita of Uzbekistan (Nessov et al., 1989; Nessov, 1995). The holotype is a left maxilla containing four teeth, but a large number of other isolated ceratopsian elements from the same formation have been referred to this taxon (Nessov et al., 1989; Nessov, 1995). Although not directly associated with the holotype, these elements correspond roughly in size, but referral is tentative at best and is solely based on cooccurrence within the same geological formation and on overall size. More compelling is that a number of elements are replicated (two maxillae, at least four partial dentaries, two basicrania, several surangulars) and all belong approximately to a single size range and bear identical morphologies. Although hardly conclusive evidence for a distinct taxon, interpreting these remains as pertaining to a single taxon is more conservative than interpreting them as deriving from

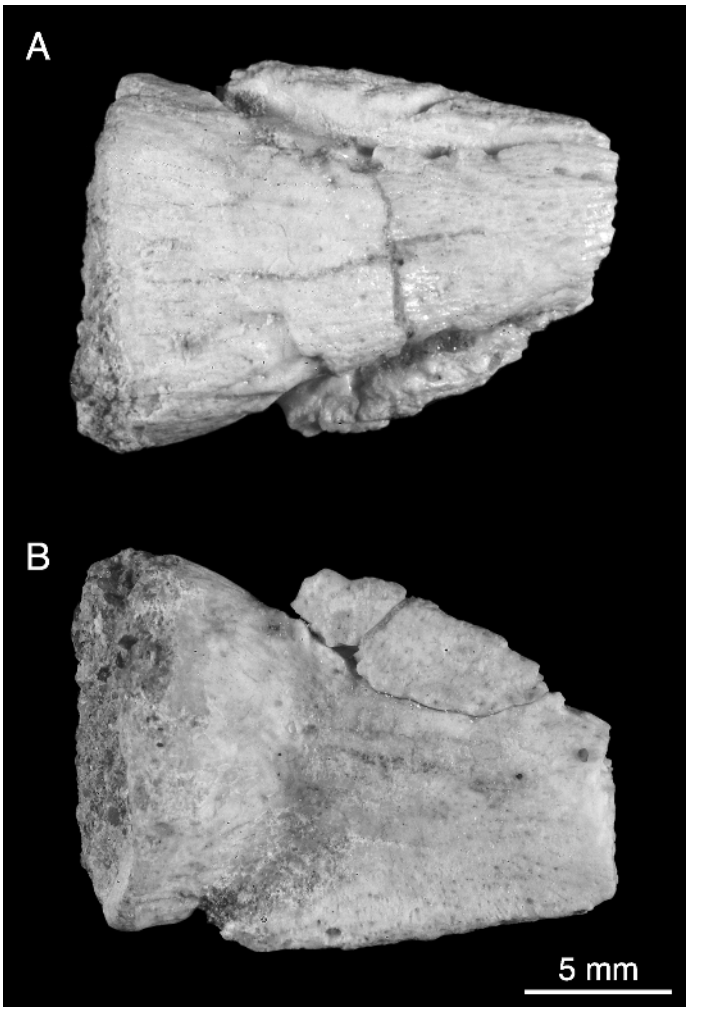

Fig. 19. Pedal ungual of the referred specimen of *Yamaceratops dorngobiensis* (IGM 100/1303) in dorsal (**A**) and ventral (**B**) views.

multiple species (Makovicky, 2002). The possibility that this material stems from juveniles, as indicated by low tooth counts in the preserved jaw elements, detracts from this argument, however, as juvenile ceratopsians often lack diagnostic characters (Sampson et al., 1997). The holotype maxilla is not diagnostic by itself, but assuming that all referred material belongs to the same taxon as the maxilla, one character may prove diagnostic. In an isolated basicranium, tentatively referred to *Asiaceratops salsopaludalis* (TsNIGRI 496/12457), a triangular process of the basioccipital fits into a corresponding gap on the posterior face of the basisphenoid on the ventral surface of the braincase. In other taxa, this suture is either flat or there is an embayment on the basisphenoid, but no corresponding process on the basioccipital. Therefore, with the caveat that its status as a monophyletic taxon has yet to be determined, *Asiaceratops* is tentatively included in the phylogenetic analysis.

Graciliceratops is based on a single immature individual (MgD I/75) comprising a partial skull and postcranium. Sereno (2000) recently reviewed the status of this taxon and separated it from *Microceratops*, which is

a *nomen dubium*. Although Sereno (2000) diagnosed *Graciliceratops* based on the slender nature of its frill and a high tibiofemoral ratio, these features are known to vary with ontogeny in the closely related *Protoceratops* (Brown and Schlaikjer, 1940b). Makovicky (2002) regarded *Graciliceratops* as a metaspecies that is provisionally diagnostic based on differential character distributions. Although similar to *Protoceratops* in most respects, it retains clawlike pedal unguals unlike any other coronosaur. It is included in the present analysis.

Several recently named taxa were not included in the analysis, because their validity is considered questionable and all may represent junior synonyms of known taxa. These taxa in question are *Bainoceratops* (Tereschenko and Alifanov, 2003), *Lamaceratops*, and *Platyceratops* (Alifanov, 2003) from the Late Cretaceous of Mongolia, and *Magnisrostris* (You and Dong, 2003) from the Bayan Mandahu locality in Inner Mongolia. The three latter taxa have been suggested as close relatives of *Bagaceratops*, but purportedly differ from the ontogenetic series of *Bagaceratops* at the Paleobiological Institute at the Polish Academy of Sciences described by Maryanska and Osmólska (1975). Unfortunately, these comparisons are insufficient, as the specimens in the Polish collections are all juveniles and very poorly preserved. Some of the characters listed by Alifanov (2003) to distinguish *Lamaceratops* and *Platyceratops* from *Bagaceratops*, such as various skull proportions, jugal horn shape, and nasal horn size and shape, are developmentally variable characteristics in ceratopsians and are observed to change with ontogeny in the closely related *Protoceratops andrewsi*. Other supposed diagnostic features of the three *Bagaceratops* relatives are artifacts of preservation (e.g., incipient orbital horn cores described in *Magnirostris*; You and Dong, 2003), are observed to vary individually among specimens of *Bagaceratops* (e.g., profile of the nasal horn), or cannot be compared to any of the Polish Academy of Sciences specimens, because the latter do not preserve the relevant parts (e.g., rostral of *Magnirostris*, frill fenestrae of *Platyceratops*). At present, all of the newly described specimens display autapomorphies of *Bagaceratops* (Makovicky, 2002) such as a fused nasal horn, presence of an accessory antorbital fenestra, a long maxillary diastema rostral to the tooth row, and a crestlike mandibular ridge on the dentary. They lack convincing character differences from *Bagaceratops*, however, that can be established across a wide range of specimens from the known growth series of this taxon. Moreover, all three taxa were collected at localities from which specimens of *Bagaceratops* have been reported, namely Khulsan (Maryanska and Osmólska, 1975), Khermeen Tsav (Maryanska and Osmólska, 1975), and Bayan Mandahu (Dong and Currie, 1993). Although it is not unreasonable to expect multiple species of *Bagaceratops* across various localities (and presumably different time intervals), a more thorough survey of characters across the range of known specimens is required to uphold the proposed generic distinctions. Therefore, we take the conservative view and consider these taxa as junior synonyms of *Bagaceratops* in this generic level analysis.

The recently named taxon *Bainoceratops* (Tereschenko and Alifanov, 2003), from the Shabarakh Usu (Flaming Cliffs) locality, was distinguished from the cooccurring *Protoceratops* based on details of vertebral morphology, including the presence of undulatory prezygapophyseal articular facets on the posterior trunk vertebrae. This feature is, however, observed in some, though not all, specimens referred to *Protoceratops* (AMNH 6424) and in the holotype of *Archaeoceratops*. It is also present in a juvenile specimen of *Montanoceratops* (MOR 542), although not in the larger holotype, suggesting that this feature is subject to individual or perhaps ontogenetic variation. The remaining vertebral features used to distinguish *Bainoceratops* are rather subtle and seem to fall within the variation observed in *Protoceratops* (P.J. Makovicky, personal obs.).

CHARACTER SAMPLING: The list of characters (appendix 1) represents an expanded version of the Xu et al. (2002) character set, which in turn was largely derived from Makovicky (2001). We have augmented those character sets with several characters developed in other recent treatments of basal

ceratopsian relationships (Sereno, 2000; Makovicky, 2002; You and Dodson, 2003), although some of these were rescored relative to their original usage. Other characters from these works were reviewed but not added, either because of overlap with characters already employed or because they were too vaguely defined to capture the morphological complexity at hand. Almost all observations were made firsthand on original specimens and personal photographs thereof.

ANALYSIS AND RESULTS: The complete matrix (appendix 2) comprises 133 characters and 20 taxa and was analyzed using the branch-and-bound parsimony algorithm in PAUP* 4.0b10 (Swofford, 1998). All characters were parsimony informative, equally weighted, and considered unordered. Branches were collapsed if their minimum length equals zero, as such branches are not supported under all optimizations. Strict consensus methods were used to assay the commonality of branching patterns among all most parsimonious trees (MPTs). The taxa *Hypsilophodon* and *Stegoceras* were used as outgroups with trees rooted on the former according to current hypotheses of ornithischian relationships (e.g., Sereno, 1999). A NEXUS version of the matrix can be downloaded from http://fm1.fieldmuseum.org/aa/Files/pmakovicky/Yamaceratops matrix.

Phylogenetic analysis resulted in four MPTs, the strict consensus of which is shown in figure 20A. *Yamaceratops* occupies a phylogenetic position as a basal neoceratopsian intermediate between *Liaoceratops* and *Archaeoceratops*. Tree length is 222 steps, the consistency index and rescaled consistency index are 0.703 and 0.566, respectively, and the retention index is 0.806. Seven unambiguous synapomorphies (chars. 29, 40, 57, 82, 84, 86, 105) unite *Yamaceratops* with higher neoceratopsians, and four unambiguous synapomorphies (chars. 28, 94, 100, 113) separate *Yamaceratops* from the clade comprising *Archaeoceratops* and more derived neoceratopsians.

Support for the phylogenetic position of *Yamaceratops* was assessed using branch support values (Bremer, 1988, 1994) (fig. 20). Despite the relatively large number of synapomorphies supporting the position of *Yamaceratops* and separating it from more derived neoceratopsians, branch support values for the most exclusive node that includes *Yamaceratops*, as well nodes immediately above and below it, are remarkably weak. Taxon deletion experiments indicate that the low support is caused by inclusion of the poorly known and questionably diagnosed *Asiaceratops salsopaludalis*. Following removal of this contentious taxon, support for the nodes at the base of Neoceratopsia below the position of *Asiaceratops* increases noticeably (fig. 20B) and the 13-step increase in tree support (the sum of all branch supports; Bremer, 1994) markedly exceeds the two-step decrease in tree length achieved through exclusion of *Asiaceratops*. This demonstrates that the low support for basal nodes in the tree is strongly linked to homoplasy and especially missing data in *Asiaceratops*, rather than being caused by more broadly distributed homoplasy across the lower nodes of the tree. In other words, instability at the *Asiaceratops*–leptoceratopsid node also adversely affects several nodes basal to it, although it has no apparent effect on more derived clades (i.e., Coronosauria and Leptoceratopsidae). Codings for *Asiaceratops* were observed on individual, isolated bones and teeth, and the problems regarding validity of this taxon and referral of isolated elements to it were discussed above. It is noteworthy that the removal of *Asiaceratops* affects neither of the diagnoses for the *Yamaceratops* + higher neoceratopsian clade and the next grouping up the tree that excludes *Yamaceratops*. This again indicates that many of the poor support values were related to missing data in *Asiaceratops* and the ambiguous character optimizations it caused, rather than homoplasy.

DISCUSSION

Yamaceratops provides important insight on the evolutionary sequence of several neoceratopsian features. All but one of the seven unambiguous synapomorphies (characters 29, 40, 82, 84, 86, 105) uniting this taxon with the *Archaeoceratops*–leptoceratopsid–coronosaur clade are located in the mandible, the dentition, and the cheek region. Indeed, three of the characters (82, 84, 86) occur on the surangular and adjacent coronoid region

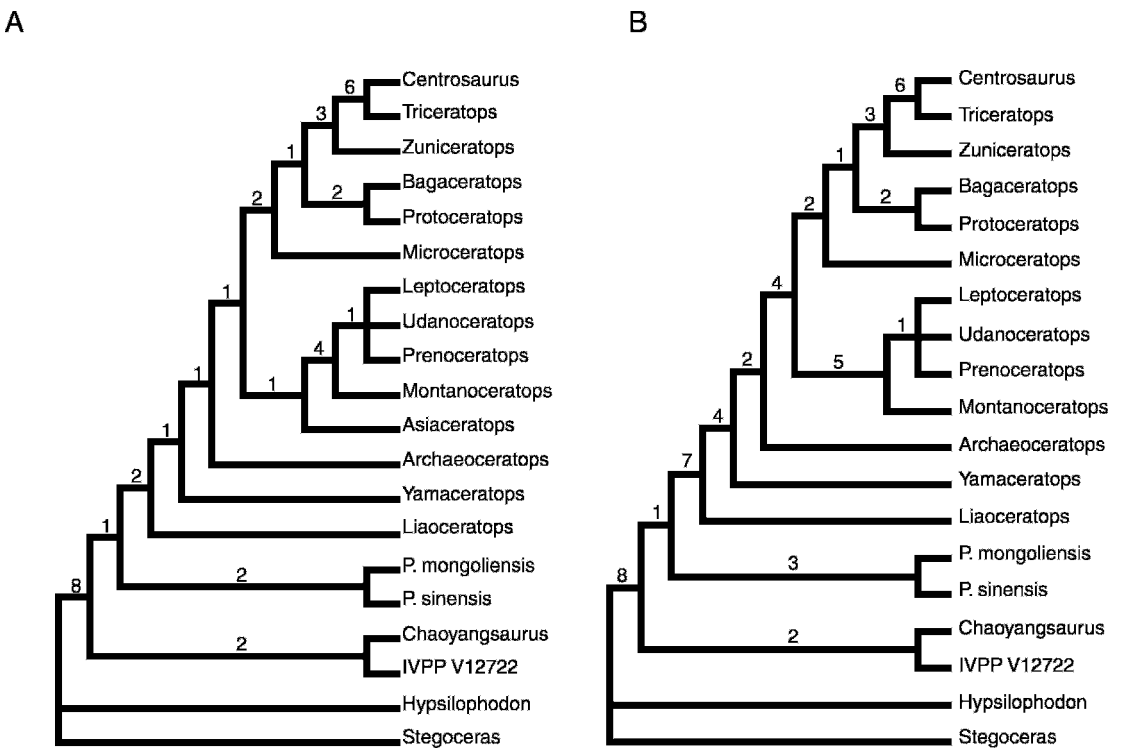

Fig. 20. **A**: Strict consensus of four most parsimonious trees (MPTs) resulting from analysis of the 133-character, 20-taxon matrix in appendix 2. **B**: Strict consensus of four MPTs from an analysis in which *Asiaceratops* was excluded. Numbers next to nodes indicate branch support (= decay index) values.

of the dentary, suggesting that they may have evolved as a functionally integrated module. Mandibular characters include modifications of the surangular such as a vertical ridge or tab that forms a lateral wall to the glenoid laterally (char. 86), covering the quadrate condyles and glenoid in lateral view. This character may be related to restricting jaw mobility to a fore and aft movement, which is the main power stroke in ceratopsian jaw mechanics (Ostrom, 1966). Another surangular synapomorphy is the presence of a distinct lateral ridge adjacent to the glenoid and dorsal to the articulation with the angular (char. 84). This ridge overhangs the surface of the mandible and extends on to the dentary in *Yamaceratops* as in *Archaeoceratops*, *Protoceratops*, and *Bagaceratops*. A more reduced ridge is present on the surangular of a juvenile *Montanoceratops* specimen (Chinnery and Weishampel, 1998), but the surangular of the adult holotype is too poorly preserved to confirm its size and presence. *Leptoceratops*, *Udanoceratops*, *Prenoceratops*, and ceratopsids bear either a very faint, rounded ridge or have no ridge at all (Chinnery, 2004). The ridge probably marks the insertion of the external jaw adductor muscles (Haas, 1955).

Another functionally related synapomorphy that makes its first appearance in *Yamaceratops* is the shift in the position of the coronoid process (char. 82). In *Liaoceratops* and more distant outgroups, the coronoid process lies caudal to the tooth row. In *Yamaceratops* and more advanced taxa, it occupies a position lateral to the caudal end of the tooth from which it is separated by a shallow sulcus. Ostrom (1964) placed great emphasis on this derived state in his analysis of ceratopsian jaw mechanics, and used simple lever models to calculate that this character transition would have provided neoceratopsians with a means to significantly amplify bite forces near the caudal end of the tooth row by

moving it closer to the jaw articulation that serves as a fulcrum.

Yamaceratops is the basalmost neoceratopsian taxon that possesses a distinct epijugal ossification (char. 29). As in other basal neoceratopsians, the epijugal is crescentic in shape and curves rostrodorsally along the edge of the jugal process. It is relatively small in *Yamaceratops* in contrast to the larger epijugals of some leptoceratopsids. An epijugal is absent in *Liaoceratops*, but is present in all other neoceratopsians (Xu et al., 2002). Another cheek region synapomorphy shared with all higher neoceratopsians is the mediolaterally expanded quadratojugal of *Yamaceratops* (char. 40), which is more derived than that of *Liaoceratops* and other outgroups in being almost concealed in lateral view rather than transversely flat.

A dental synapomorphy of *Yamaceratops* and more derived neoceratopsians is the flattening along the mesial and distal faces of the roots to accommodate the expanded crowns of the adjacent unerupted teeth (char. 105). These flattened areas make the root wider bucco-lingually than antero-posteriorly. In more advanced neoceratopsians, shallow grooves are present along mesial and distal edges of the teeth and may be a precursor to the bifid division seen in ceratopsid roots. *Yamaceratops* also displays more strongly developed primary ridges on teeth in the middle and posterior sections of the tooth rows relative to *Liaoceratops*, but we have not created a separate state to capture this distinction here. Full development of primary ridges throughout the tooth row is observed in the leptoceratopsid–coronosaur radiation.

The only derived character state transformation diagnosing the *Yamaceratops* and higher neoceratopsian clade unrelated to the feeding apparatus is the exclusion of the basioccipital from the floor of the foramen magnum (char. 57). In most neoceratopsian taxa, the exoccipitals meet on the floor of the foramen magnum and contribute the dorsal part of the large and spherical occipital condyle. This condition is not observed in *Liaoceratops*, in which the basioccipital still forms a minor, but restricted, contribution to the foramen magnum. Although the occipital region is not well preserved in the holotype of *Yamaceratops*, the suture between the exoccipitals is apparent on the floor of the foramen magnum. Their condylar contributions appear to be lost, however.

The discovery of *Yamaceratops* augments the recent descriptions of other basal neoceratopsian taxa and improves our knowledge of early neoceratopsian anatomy and broadens the understanding of the early evolution and diversity of the clade. The addition of yet another taxon near the base of Neoceratopsia serves to establish the polarity for a number of derived structures diagnosing the clade. Some of these could only be observed in the well-preserved specimens of *Liaoceratops*, but their polarity was uncertain given the missing or poorly preserved parts of the *Archaeoceratops* holotype and the lack of relevant cranial parts in the basal leptoceratopsids *Montanoceratops* and *Asiaceratops* as well as in the basal coronosaur *Graciliceratops*.

For example, the rostral process of the postorbital is bifid and receives the caudal tip of the postorbital on the temporal bar of *Liaoceratops* (char. 114, state 1). The temporal bar is poorly preserved in *Archaeoceratops*; however, You and Dodson (2003) reconstructed the squamosal with almost no rostral process and a flat suture with the postorbital, a condition unlike that observed in any other ceratopsian. The rostral process of the squamosal appears bifid in the leptoceratopsids *Montanoceratops* and *Leptoceratops*, but is unknown in *Asiaceratops* and *Microceratops* and is modified in other coronosaurs. Until the observation of a bifid temporal process of the squamosal in *Yamaceratops*, the polarity and optimization of the character were unsure, drawing into question the distribution of the more complex suture pattern that is now interpreted as a coronosaurian synapomorphy.

Unfortunately the parietal margin of the frill is not preserved in *Yamaceratops*, but the squamosal edge is very reminiscent of the condition in *Liaoceratops* in both its robustness, its arcuate curvature toward the midline, and in the shape of the concave posterolateral corner to the supratemporal muscle chamber. This squamosal morphology persists in *Leptoceratops* and optimizes as plesiomorphic for noncoronosaurian neoceratopsians. In

Liaoceratops, the caudal edge of the frill is robust and heavily pitted by muscle insertions, indicating that the frill served as a platform for large jaw adductors. The strong similarities in squamosal shape between *Yamaceratops* and *Liaoceratops* noted above suggest that the frill probably served the same function in the former taxon.

Historically, the frill of ceratopsians has been interpreted as either a defensive structure (Hatcher et al., 1907) or, more commonly, as an expanded anchorage for hypertrophied jaw musculature (Haas, 1955; Ostrom, 1964). More recently, the predominant view, based on studies of ceratopsid diversity (Horner et al., 1992; Sampson, 1995), ontogeny (Sampson et al., 1997), and disparity, has been to view frills as display structures related to species recognition and mate competition (Sampson, 1999). The uniform short, robust morphology of basal neoceratopsian frill morphologies suggests, however, that the evolution of the frill as a display structure was a secondary exaptation, most likely evolving within the coronosaurian radiation.

Despite the long list of synapomorphies positing *Yamaceratops* between *Liaoceratops* and *Archaeoceratops*, this position is not without conflict. Several characters states, such as the unkeeled shape of the rostral and the shape of the jugal, require additional steps to be accommodated on the MPTs. Although the rostral is keeled in *Archaeoceratops* and is now known to be keeled in at least one well-preserved *Liaoceratops* specimen (*contra* Xu et al., 2002; see You and Dodson, 2003), it is clearly unkeeled in *Yamaceratops*, introducing ambiguity to the optimization of this character. Whether this particular trait, which is among a handful of characters relevant to current disagreements regarding the phylogenetic position of *Chaoyangsaurus* (Makovicky et al., 2004), displays some level of ontogenetic or individual variation will require the discovery of further specimens of both *Yamaceratops* and *Liaoceratops*.

This particular character also underscores the need to review character inclusion criteria as novel combinations of states are recognized. A keeled morphology of the predentary was previously assumed to be codependent with rostral morphology by one of us and was therefore excluded as a separate character from earlier analyses (e.g., Makovicky, 2001). *Yamaceratops* demonstrates, however, that a keeled predentary could cooccur with an unkeeled rostral, thus corroborating the assumed independence between these characters in other analyses of ceratopsian relationships (Sereno, 2000).

Other increments in tree length are caused by the observation of features in *Yamaceratops* that were previously considered unique attributes of *Liaoceratops*, such as the presence of a lateral tubercle on the angular just distal to the articular articulation (char. 74) or the above-mentioned jugal shape character (char. 28). A triangular jugal morphology with a deep suborbital ramus that is dorsoventrally as wide or wider than the subtemporal ramus has been proposed as a ceratopsian synapomorphy. Nevertheless, both *Yamaceratops* and *Liaoceratops* share a jugal morphology in which the infratemporal ramus is deeper than the orbital one in contrast to *Chaoyangsaurus*, psittacosaurids, and higher neoceratopsians. The relatively small laterotemporal fenestra is delimited by wide postorbital and infratemporal processes of the jugal, quite unlike the expanded and very deep infratemporal fenestra of psittacosaurids and *Chaoyangsaurus*.

A similar increase in homoplasy following the introduction of a new taxon was noted by Xu et al. (2002) in their description of *Liaoceratops*. Certain features previously thought to be restricted to psittacosaurids were observed in *Liaoceratops*, causing an increase in tree length, but also providing valuable insight into the mosaic evolution of early ceratopsians. Such patterns of character evolution in which derived characters diagnosing paraphyletic grades of the tree due to secondarily loss or overprinting are not as pronounced with the discovery of *Yamaceratops*, whose addition to the matrix only leads to a three-step increment in homoplasy (unkeeled rostral, jugal shape, and angular tubercle). Nevertheless, this mode of character evolution may be prevalent in the early evolutionary history of ceratopsians. Another potential example from this dataset may be the brevirostrine morphology of *Psittacosaurus* and the chaoyangsaurids (Zhao et al., in press). If

chaoyangsaurids are the most basal ceratopsians, as suggested by two of the MPTs, the brevirostrine condition may optimize as a diagnostic feature of all ceratopsians that is subsequently reversed in neoceratopsians.

These complex character distributions along with the relatively long internodes between basal neoceratopsian taxa on the MPTs hints at a wider, undiscovered diversity of such forms. Topologically, the diagnostic characters supporting these branches are largely concentrated in skull parts related to feeding. Determining whether such topological concentrations of synapomorphies reflect tightly integrated modules of characters evolving rapidly in concert or a slower, more incremental accrual will require discovery of more basal neoceratopsians, as well as insights into ontogenetic series.

CONCLUSIONS

Until recently, diagnostic remains of Early Cretaceous neoceratopsians have been very scarce. A new neoceratopsian taxon, *Yamaceratops dorngobiensis*, is described herein. It is probably Albian in age and adds to our knowledge of early neoceratopsian diversity and evolutionary history. *Yamaceratops* provides definitive evidence for an epijugal ossification early in the history of this clade and confirms a pattern of rapid, progressive acquisition of neoceratopsian synapomorphies, especially in the mandible, during the early history of the group. Similarities to *Liaoceratops* in squamosal morphology suggest that the frill served as a platform for enlarged jaw adductor musculature early in the history of the group, and other similarities in cheek morphology suggest that evolution of the jaw adductor chamber was more divergent between psittacosaurids and neoceratopsians than previously recognized.

Early neoceratopsian history was marked by mosaic character evolution as noted by Xu et al. (2002), and *Yamaceratops* underscores that pattern for a number of features, in spite of its otherwise intermediate appearance. In addition to the jugal morphology already mentioned, the absence of a keel on the rostral can be added to a pattern of characters that appeared to evolve in parallel or undergo some independent losses early in the history of the clade. Clearly, much remains to be discovered about neoceratopsian origins and diversification as more complete specimens and new taxa are discovered.

ACKNOWLEDGMENTS

We thank the 1991 and 2002–2003 Mongolian American Expedition crews who discovered the specimens of *Yamaceratops* published herein. Julia Clarke discovered and collected the referred specimen IGM 100/1303. Jane Shumsky (AMNH) and Lisa Herzog (TFM) carefully prepared the published material. Specimen photography by John Weinstein (TFM) and digital processing of the photos by Mick Ellison (AMNH) significantly improved the quality of this paper. We thank Brenda Chinnery-Allgeier and Michael Ryan for thoughtful reviews of the manuscript. Research presented herein was supported by an award from the National Science Foundation (EAR 0418648) to P.J.M.

REFERENCES

Alifanov, V.R. 2003. Two new dinosaurs of the infraorder Neoceratopsia (Ornithischia) from the Upper Cretaceous of the Nemegt depression, Mongolian People's Republic. Paleontological Journal 37(5): 524–534.

Benton, M.J. 2000. Conventions in Russian and Mongolian paleontological literature. *In* M.J. Benton, M. Shishkin, D.M. Unwin and E. Kurochkin (editors), The Age of Dinosaurs in Russia and Mongolia: xvi–xxxix. Cambridge: Cambridge University Press.

Bremer, K. 1988. The limits of amino-acid sequence data in angiosperm phylogenetic reconstruction. Evolution 42(4): 795–803.

Bremer, K. 1994. Branch support and tree stability. Cladistics 10: 295–304.

Brochu, C. 1996. Closure of neurocentral sutures during crocodilian ontogeny: implications for maturity assessment in fossil archosaurs. Journal of Vertebrate Paleontology 16: 49–62.

Brown, B., and E.M. Schlaikjer. 1940a. A new element in the ceratopsian jaw with additional notes on the mandible. American Museum Novitates 1092: 1–13.

Brown, B., and E.M. Schlaikjer. 1940b. The structure and relationships of *Protoceratops*. Annals of the New York Academy of Sciences 40: 133–266.

Chinnery, B. 2004. Description of *Prenoceratops pieganensis* gen. et sp. nov. (Dinosauria: Neoceratopsia) from the Two Medicine Formation of Montana. Journal of Vertebrate Paleontology 24(3): 572–590.

Chinnery, B.J., and D.B. Weishampel. 1998. *Montanoceratops cerorhynchus* (Dinosauria: Ceratopsia) and relationships among basal neoceratopsians. Journal of Vertebrate Paleontology 18(3): 569–585.

Currie, P.J., and D.A. Eberth. 1993. Paleontology, sedimentology and paleoecology of the Iren Dabasu Formation (Upper Cretaceous), Inner-Mongolia, People's Republic of China. Cretaceous Research 14(2): 127–144.

Dong, Z.-M., and Y. Azuma. 1997. On a Primitive Neoceratopsian from the Early Cretaceous of China *In* Z.-M. Dong (editor), Sino-Japanese Silk Road Dinosaur Expedition: 68–89. Beijing: China Ocean Press.

Dong, Z.M., and P.J. Currie. 1993. Protoceratopsian embryos from Inner Mongolia, People's Republic of China. Canadian Journal of Earth Sciences 30(10–11): 2248–2254.

Edmund, A.G. 1960. Tooth replacement phenomena in the lower vertebrates. Royal Ontario Museum, Life Sciences Division Contributions 52: 1–190.

Galton, P.M. 1974. The ornithischian dinosaur *Hypsilophodon* from the Wealden of the Isle of Wight. Bulletin of the British Museum (Natural History), Geology 25(1): 1–152c.

Gilmore, C. 1917. *Brachyceratops*, a new ceratopsian dinosaur from the Two Medicine Formation of Montana with notes on associated reptiles. United States Geological Survey Professional Paper 103: 1–45.

Gilmore, C. 1933. On the dinosaurian fauna of the Iren Dabasu Formation. Bulletin of the American Museum of Natural History 67: 23–78.

Haas, G. 1955. The jaw musculature in *Protoceratops* and other ceratopsians. American Museum Novitates 1729: 1–24.

Hatcher, J.B., O.C. Marsh, and R.S. Lull. 1907. The Ceratopsia. U. S. Geological Survey, Monograph 49: 1–300.

Horner, J.R., D.J. Varricchio, and M.B. Goodwin. 1992. Marine transgressions and the evolution of Cretaceous dinosaurs. Nature 358(6381): 59–61.

Jerzykiewicz, T., and D.A. Russell. 1991. Late Mesozoic stratigraphy and vertebrates of the Gobi Basin. Cretaceous Research 12: 345–377.

Khand, Y., D. Badamgarav, Y. Ariunchimeg, and R. Barsbold. 2000. Cretaceous system in Mongolia and its depositional environments *In* H. Okada and N.J. Mateer (editors), Cretaceous Environments of Asia: 49–79. Amsterdam: Elsevier.

Makovicky, P.J. 2001. A *Montanoceratops cerorhynchus* (Dinosauria: Ceratopsia) braincase from the Horseshoe Canyon Formation of Alberta. *In* D. Tanke and K. Carpenter (editors), Mesozoic vertebrate life, new research inspired by the paleontology of Philip J. Currie: 243–262. Bloomington, IN: Indiana University Press.

Makovicky, P.J. 2002. Taxonomic revision and phylogenetic relationships of basal Neoceratopsia (Dinosauria: Ornithischia). 288 + X pp. Ph.D. dissertation, Columbia University: New York City.

Makovicky, P.J., M.A. Norell, and X. Xu. 2004. Basal ceratopsians from China and Mongolia with a reappraisal of ceratopsian relationships. Journal of Vertebrate Paleontology 24(suppl. to 3): 88A.

Maryanska, T., and H. Osmólska. 1975. Protoceratopsidae (Dinosauria) of Asia. Palaeontologia Polonica 33: 133–181.

Nessov, L.A. 1995. Dinosaurs of northern Eurasia: new data about assemblages, ecology and palaeobiogeography. St. Petersburg: University of Saint Petersburg, 156 pp.

Nessov, L.A., L.F. Kaznyshkina, and G.O. Cherepanov. 1989. Ceratopsian dinosaurs and crocodiles of the middle Mesozoic of Asia. *In* T.N. Bogdanova and L.I. Kozhatsky (editors), Theoretical and applied aspects of modern paleontology: 142–149. Leningrad: Nauka.

Osmólska, H. 1986. Structure of nasal and oral cavities in the protoceratopsid dinosaurs (Ceratopsia, Ornithischia). Acta Palaeontologica Polonica 31(1–2): 145–157.

Ostrom, J.H. 1964. A functional analysis of the jaw mechanics in the dinosaur *Triceratops*. Postilla 88: 1–35.

Ostrom, J.H. 1966. Functional morphology and evolution of the ceratopsian dinosaurs. Evolution 20: 290–308.

Ryan, M.J., and P.J. Currie. 1998. First report of protoceratopsians (Neoceratopsia) from the Late Cretaceous Judith River Group, Alberta, Canada. Canadian Journal of Earth Sciences 35(7): 820–826.

Sampson, S.D. 1995. Two new horned dinosaurs from the Upper Cretaceous Two Medicine Formation of Montana; with a phylogenetic analysis of the Centrosaurinae (Ornithischia:Ceratopsidae). Journal of Vertebrate Paleontology 15(4): 743–760.

Sampson, S.D. 1999. Sex and destiny: the role of mating signals in speciation and macroevolution. Historical Biology 13: 173–197.

Sampson, S.D., M.J. Ryan, and D.H. Tanke. 1997. Craniofacial ontogeny in centrosaurine dinosaurs (Ornithischia: Ceratopsidae): taxonomic and behvioral implications. Zoological Journal of the Linnean Society 121: 293–337.

Schumacher, G. 1973. The head muscles and hyolaryngeal skeleton of turtles and crocodilians. *In* C. Gans and T. Parsons (editors), Biology of the Reptilia: 101–199. New York: Academic Press.

Sereno, P.C. 1986. Phylogeny of the bird-hipped dinosaurs (order Ornithischia). National Geographic Research 2: 234–256.

Sereno, P.C. 1999. The evolution of dinosaurs. Science 284(5423): 2137–2147.

Sereno, P.C. 2000. The fossil record, systematics and evolution of pachycephalosaurs and ceratopsians from Asia. *In* M. Benton, M. Shishkin, D. Unwin and E. Kurochkin (editors), The Age of Dinosaurs in Russia and Mongolia: 480–516. Cambridge: Cambridge University Press.

Shuvalov, V.F. 2000. The Cretaceous stratigraphy and palaeobiogeography of Mongolia. *In* M.J. Benton, M. Shishkin, D.M. Unwin and E. Kurochkin (editors), The Age of Dinosaurs in Russia and Mongolia: 236–278. Cambridge: Cambridge University Press.

Sternberg, C.M. 1951. Complete skeleton of *Leptoceratops gracilis* Brown from the Upper Edmonton Member on Red Deer River, Alberta. National Museum of Canada Bulletin, Annual Report (1949–50) 123: 225–255.

Swisher, C.C., X.L. Wang, Z.H. Zhou, Y.Q. Wang, F. Jin, J.Y. Zhang, X. Xu, F.C. Zhang, and Y. Wang. 2002. Further support for a Cretaceous age for the feathered-dinosaur beds of Liaoning,China: New Ar-40/Ar-39 dating of the Yixian and Tuchengzi formations. Chinese Science Bulletin 47(2): 135–138.

Swofford, D. 1998. PAUP*. Phylogenetic analysis using parsimony (*and other methods), 4. Sunderland, MA: Sinauer Associates.

Tang, F., Z.X. Luo, Z.H. Zhou, H.L. You, J.A. Georgi, Z.L. Tang, and X.Z. Wang. 2001. Biostratigraphy and palaeoenvironment of the dinosaur-bearing sediments in Lower Cretaceous of Mazongshan area, Gansu Province, China. Cretaceous Research 22(1): 115–129.

Tereschenko, V.S., and V.R. Alifanov. 2003. *Bainoceratops efremovi*, a new protoceratopid dinosaur (Protoceratopidae, Neoceratopsia) from the Bain-Dzak locality (south Mongolia). Paleontological Journal 37(3): 293–302.

Xu, X., P.J. Makovicky, X.L. Wang, M.A. Norell, and H.L. You. 2002. A ceratopsian dinosaur from China, and the early evolution of Ceratopsia. Nature 416(6878): 314–317.

You, H.L., and P. Dodson. 2003. Redescription of the neoceratopsian dinosaur *Archaeoceratops* and early evolution of Neoceratopsia. Acta Palaeontologica Polonica 48(2): 261–272.

You, H.L., and Z.M. Dong. 2003. A new protoceratopsid (Dinosauria: Neoceratopsia) from the Late Cretaceous of Inner Mongolia, China. Acta Geologica Sinica—English Edition 77(3): 299–303.

Zhao, X., Z. Cheng, and X. Xu. 1999. The earliest ceratopsian from the Tuchengzi Formation of Liaoning, China. Journal of Vertebrate Paleontology 19(4): 681–691.

Zhao, X.J., Z.W. Cheng, X. Xu, and P.J. Makovicky. In press. A new ceratopsian from the Upper Jurassic Houcheng Formation of Hebei, China. Acta Geologica Sinica—English Edition.

APPENDIX 1

Character List

Reference abbreviations: C&W, Chinnery and Weishampel, 1998; S, Sereno, 2000; Y&D, You and Dodson, 2003. Numbers following shorthand citations refer to the character number employed in the original study.

1. Head size small relative to body (0) or large relative to body (1).
2. Head shape in dorsal view: elongate, ovoid (0), or triangular, wide over jugals (1).
3. Orbit diameter more than 20% of skull length (0) or less (1).
4. Preorbital region more than 40% (0) or less than 40% (1) the length of the skull.
5. Tip of rostral low and level with maxillary tooth row (1) or raised and dorsal to maxillary tooth row (1).
6. Rostral bone forming beak absent (0) or present (1).
7. Rostral ventral (buccal) process absent (0) or present (1).
8. Anterior face of rostral round, convex (0) or sharply keeled (1).
9. Premaxillary palatal region flat in ventral view (0) or vaulted dorsally (1).
10. Relative height of premaxilla (snout) to orbital region low (0) or deep (1).
11. Premaxilla–prefrontal contact absent (0) or present (1).
12. Convex buccal process anterior to maxillary tooth row formed by premaxilla or premaxilla

and maxilla absent (0) or present (1). (Similar but not identical to Y&D 8).
13. Premaxilla–maxilla buccal margin relatively straight in ventral view, tooth rows/buccal margins converge rostrally (0) or buccal margin sinuous in ventral view, with premaxillary palatal region flaring widely rostral to tooth row (1).
14. Anterior end of the nasal (internarial bar) above (0) or below and far rostral to the external naris (1).
15. Nares position close to buccal margin (0) or dorsal, away from buccal margin (1) or very far dorsal, level with upper part of orbit (2).
16. Ventral border of external nares significantly below (0), about the level of (1), or significantly above (2) lower rim of infratemporal fenestra.
17. Large depression excavating premaxilla anteroventral to naris absent (0) or present (1).
18. Nasal horn absent (0), small (1), or large (2).
19. Naris width (excluding narial depression) less than 10% of skull length (0) or more than 10% of skull length (1).
20. Position of choana on palate: anterior to maxillary tooth row (0) or level with maxillary tooth row (1).
21. Maxillae from opposite sides separated by vomers at anterior border of the internal choanae (0) or maxillae contact each other anterior to choanae in palatal view and tip of vomer obscured from view (1).
22. Dentigerous margin of maxilla straight (0) or ventrally convex (1).
23. Antorbital fossa reduced or absent (0) or large and triangular or rounded in shape (1).
24. Eminence or tubercle on the rim of the buccal emargination of the maxilla near the junction with the jugal absent (0) or present (1).
25. Palpebral free, articulating with lacrimal (0) or fused to orbital margin (1).
26. Jugal–lacrimal contact reduced (0) or expanded (1).
27. Jugal horns absent (0) or present and laterally directed (1) or present and ventrally directed (2).
28. Jugal suborbital ramus not as deep as subtemporal ramus (0) or suborbital ramus as deep or deeper than orbital ramus (1) (S 5).
29. Epijugal ossification absent (0) or present (1).
30. Epijugal position on jugal: along dorsal edge of horn (epijugal trapezoidal) (0) or capping end of horn (epijugal conical) (1).
31. Orbital horns absent (0) or present (1).
32. Postorbital inverted L-shaped (0) or triangular and platelike (1).
33. Postorbital with dorsal part rounded and overhanging lateral edge of supratemporal fenestra (0) or with concave dorsal shelf bordering supratemporal fenestra (1).
34. Laterotemporal fenestra with postorbital participation in margin (0), postorbital excluded from margin (1), or jugal–squamosal contact very wide and postorbital situated far from fenestra (2).
35. Laterotemporal fenestra width more than 10% of skull length (0) or less than 10% of skull length (1) (C&W).
36. Squamosal subtriangular in lateral view (0) or T-shaped, with postquadratic process (1).
37. Temporal process of squamosal simple (0) or deeply bifurcate around temporal process of postorbital (1).
38. Posterior edge of squamosal angled anteromedially (0) or posteromedially, squamosal contributing lateral portion of frill margin (1).
39. Temporal bars of squamosals parallel (0) or posteriorly divergent (1).
40. Quadratojugal mediolaterally flattened (0) or transversely expanded and triangular in coronal section (1) or triangular in coronal section, but with slender anterior prong articulating with jugal (2).
41. Quadrate shaft anteriorly convex in lateral view (0) or straight (1).
42. Elongate parasagittal process of the palatine absent (0) or present (1).
43. Ectopterygoid exposed in palatal view (0) or reduced and concealed in palatal view (1).
44. Ectopterygoid contacts jugal (0) or ectopterygoid reduced and restricted to contact with maxilla (1).
45. Pterygopalatine foramen (modified suborbital fenestra) large (0) or diminutive (1).
46. Ventral ridge on mandibular process of pterygoid defining ''Eustachian canal'' absent (0) or present (1).
47. Pterygoid–maxilla contact at posterior end of tooth row absent (0) or present (1).
48. Prominent posterior midline process on pterygoid absent (0) or present (1).
49. Pterygoid mandibular process short (0) or long, extending well below maxillary tooth row (1).
50. Pterygoid mandibular process formed only by pterygoid (0) or jointly by pterygoid and ectopterygoid (1).
51. Parieto-frontal contact flat (0), depressed (1), or invaginated by fontanelle (2).
52. Parieto-squamosal frill absent (0) or parietal frill less than 70% of basal length of skull (1) or more than 70% of basal length (2).
53. Dorsal edge of squamosal temporal bar curves medially at the posterior end, arcing confluently into posterior frill margin (0) or dorsal

edge of squamosal meets posterior margin of frill at acute angle (1).
54. Frill solid (0) or fenestrated near posterior margin (1).
55. Distinctive indentation on midline of the posterior parietals present (0) or absent (1).
56. Epoccipital ossifications/frill scallops absent (0) or present (1).
57. Basioccipital participates in foramen magnum (0) or basioccipital is excluded from foramen magnum and exoccipitals form less than one-third of condyle (1) or exoccipitals form about half or more of occipital condyle (2).
58. Basioccipital excluded from basal tubera by basisphenoid and limited to occipital midline (0) or basioccipital tubera present (1).
59. Basipterygoid process orientation anterolateral (0), ventral (1), or posteroventral (2) when braincase is oriented with condyle pointing posteriorly.
60. Basioccipital tubera flat, in plane with basioccipital plate (0) or everted posterolaterally, forming lip beneath occipital condyle (1).
61. Notch between posteroventral edge of basisphenoid and base of basipterygoid process deep (0) or notch shallow and base of basipterygoid process close to basioccipital tubera (1).
62. Exoccipital with three exits for cranial nerves X–XII near occipital condyle (0) or with two exits (1).
63. Exoccipital–quadrate separated by ventral flange of squamosal (0) or in contact (1).
64. Paroccipital processes deep (height $\geq$ ½ length) (0) or significantly narrower (1).
65. Supraoccipital participates in dorsal margin of foramen magnum (0) or excluded from foramen magnum by exoccipitals (1).
66. Supraoccipital anteriorly inclined relative to basioccipital (0) or in same plane as posterior face of basioccipital (1).
67. Supraoccipital shape tall, triangular (0) or wider than tall, trapezoid (1) or square (2).
68. Tip of predentary shallow (0) or scooplike (1).
69. Predentary with rounded anterior margin and distally broad posteroventral process (0) or with pointed anterior margin and distally narrow posteroventral process (1).
70. Predentary less than two-thirds of dentary length (0) or equal to or more than two-thirds of dentary length (1).
71. Predentary buccal margin sharp (0) or with a rounded, beveled edge (1) or with grooved, triturating edge (2).
72. Tip of dentary smooth (0) or grooved dorsally for reception of the lateral process of the predentary (1) or bears large pit for reception of the lateral process of the predentary (2).
73. Dentary symphyseal area small (0) or large, forming strong immobile bond with participation of splenial (1).
74. Diastema between predentary and first dentary tooth absent (0) or present (1).
75. Ventral margin of dentary curved (0) or straight (1) in lateral view.
76. Dentary flange absent (0) or present along ventral edge (1).
77. Prominent medial expansion of the central mandible in the middle of the tooth row formed by wide Meckelian groove separating tooth-bearing part of the jaw from external surface absent (0) or present (1).
78. Labial face of dentary smooth below tooth row (0) or rugose and sculpted (1).
79. Contact between dentary and prearticular absent (0) or present (1).
80. Posterior end of splenial simple or with shallow dent (0) or with bifid overlap of angular (1).
81. Distal end of coronoid process rounded (0) or with anterior expansion (1).
82. Coronoid process positioned close to main axis of dentary and posterior to tooth row (0) or set lateral to tooth row, and end of tooth row covered by anterior part of coronoid process (1) or tooth row level with posterior edge of coronoid process (2).
83. Coronoid straplike and with subequal depth throughout (0) or with lobate, highly expanded dorsal end much deeper than ventral end that slots between splenial and dentary (1) (S37).
84. Surangular without distinct lateral ridge or shelf overhanging angular (0) or shelf/ridge present (1). This probably served for insertion of jaw adductor musculature (Ostrom, 1964).
85. Lateral surface of surangular flat or only weakly convex (0) or with pronounced laterally convex curvature (in the transverse plane) between the coronoid process and glenoid region (1).
86. Tab on surangular forming lateral wall to glenoid cotyle absent (0) or present (1).
87. Angular without one or more small, lateral tubercles along ventral rim below glenoid articulation (0) or tubercles present (1) (Xu et al., 2002).
88. Lateral surface of angular flat or slightly convex (0) or angular bears a raised emargination along posteroventral margin of mandible, lateral surface distinctly concave (1).
89. Angular–surangular–dentary contact triradiate (0) or surangular with long ventral process overlapping angular, dentary–surangular and

angular–surangular sutures form acute angle on lateral face of mandible (1).
90. Mandibular glenoid narrow and flush with medial margin of surangular flange in dorsal view (0) or glenoid region medially expanded and forming lingual process in dorsal view (1).
91. Surface of prearticular and articular below glenoid smooth (0) or with wide, semicircular ventral process near medial face of glenoid (1).
92. Retroarticular process long (0) or short or absent (1).
93. Three or more teeth in premaxilla (0) or two teeth in premaxilla (1) or 1 tooth in premaxilla (2) or premaxilla edentulous (3).
94. Premaxillary teeth with carinae, and in some cases serrations (0) or premaxillary teeth peglike, crown without carinae (1) (overlaps with S9).
95. Teeth with single roots (0) or with double roots (1).
96. Cheek teeth spaced (0) or closely apressed with determinate eruption and replacement pattern (1).
97. Teeth occlude at an oblique angle (0) or at a vertical angle (1) or at a vertical angle, but dentary teeth have a horizontal shelf on the labial face (2).
98. Teeth without distinct median primary ridge (0) or with very weak and wide median ridge on at least some maxillary teeth (1) or all maxillary and dentary teeth with distinct primary ridge (2). Varies with ontogeny, coded on adults.
99. Base of primary ridge confluent with the cingulum on maxillary teeth (0) or base of primary ridge set back from cingulum, which forms a continuous ridge at the crown base (1).
100. Pronounced cingula on cheek teeth absent (0) or present (1).
101. Tooth row double, with only one replacement tooth present at a time (0) or battery-like with multiple ($\geq$ 3) rows of replacement teeth (1).
102. Both lingual and buccal sides of teeth covered with enamel (0) or enamel restricted to lateral side of maxillary and medial side of dentary teeth (1).
103. Dentary tooth crowns with continuous, smooth root crown transition (0) or bulbous expansion at root-crown transition on labial side of tooth, sometimes worn to form notch or shelf (1).
104. Number of alveoli in dentary less than 20 (0) or more than 20 (1).
105. Cheek teeth with cylindrical roots (0) or roots with mesial and distal faces flattened to slightly grooved (1).
106. Tooth crowns radiate or pennate in lateral view (0) or crowns ovate in lateral view (1).
107. Atlas intercentrum semicircular (0) or disc shaped (1).
108. Atlas intercentrum not fused to odontoid (0) or fused (1).
109. Atlas neurapophyses free (0) or fused to intercentrum/odontoid (1).
110. Axial neural spine low (0) or tall and hatchet-shaped (1) or elongate and posteriorly inclined (2).
111. The neural spine of the axis anteroposteriorly short (0) or long, extending caudally to the posterior end of the centrum of the succeeding cervical (1).
112. Syncervical absent (0), partially fused (centra but not arches) (1), or completely coossified (2).
113. Dorsal vertebrae with flat articulations on zygapophyses (0) or tongue and grooves articulations on zygapophyses (1).
114. Number of sacrals: five (0) or six (1) or seven (2) or eight or more (3).
115. Outline of sacrum defines rectangle or hourglass in dorsal view (0) or oval in dorsal view (1).
116. Caudal neural spines short and inclined (0) or tall and straight (1).
117. Tail terminates with series of cylindrical caudals that are devoid of neural spines and chevrons (0) or neural spines and chevrons persist virtually to the end of tail (1) (S43).
118. Distal chevrons with lobate expanded shape (0) or rodlike (1).
119. Clavicles absent (0) or present (1).
120. Scapula distinctly curved in sagittal view (0) or relatively flat (1).
121. Scapular blade at acute angle relative to glenoid (0) or almost perpendicular to glenoid (1).
122. Coracoid with smooth, arcuate anterior portion (0) or bearing large anterolateral ridge near confluence of anterior and ventral margins (1).
123. Olecranon process relatively small (0) or enlarged ($\geq$ 1/3 of ulnar length) (1).
124. More than two distal carpals (0) or less than two distal carpals (1).
125. Manus much smaller than pes (0) or closer to pes in size (1).
126. Shaft of postpubis round (0) or mediolaterally flattened, bladelike (1) in cross section.
127. Postpubis long and ventrally oriented (0) or short and posteriorly directed (1).
128. Prepubis short and rod-shaped (0) or long and flared at anterior end (1).

129. Ischial shaft straight (0) or with posterodorsally convex curvature (1).
130. Femoral fourth trochanter large and pendant (0) or reduced (1).
131. Tibio-femoral ratio more than one (0) or less than one (1).
132. Foot gracile with long, constricted metatarsus, elongate phalanges (0) or short and uncompressed, all phalanges wider than long (1).
133. Pedal unguals pointed (0) or rounded, hooflike (1).

APPENDIX 2
CHARACTER-TAXON MATRIX

	1111111111222222222233333333334444444 12345678901234567890123456789012345678901234
Hypsilophodon foxi	00000???0000000000000001000000-000000000000000?
Stegoceras validus	00000???0000000000000000011000-0??010010?00000
Archaeoceratops oshimai	11001011110110100002?0100011100?110??011????
Asiaceratops salsopaludalis	????1???1?????1?0????01??????????????????????
Bagaceratops rozhdestvenskyi	11001?111101?01?01?0101000111101010101121100?
Chaoyangsaurus youngi	11011000?2?00?120????0?1??010?????0????0????0
Centrosaurus apertus	11101011110110011211100011211111021101111211 1
Leptoceratops gracilis	11001111110110120000111000111001100011011002?
Graciliceratops mongoliensis	1100?????????????????0???????1????????101111????
Montanoceratops cerorhynchus	1????????1????1????0?01?0?1?10011??011?11????
Protoceratops andrewsi	11001111110100120100101000111101010101121 1001
Psittacosaurus mongoliensis	11011000111011220001100100110?000000000000100
Triceratops horridus	11101111110010011211100011211111021101111211 1
Udanoceratops tshizhovi	1??011111?0???1?00?0?1????1110?????????11????
Zuniceratops christopheri	???????1?????????0???0????1???1?????????????
Liaoceratops yanzhiguouensis	?100101111101010000010110010-01010011001?000
Psittacosaurus sinensis	11011100111011220002?00000110-000000000002?00?
IVPP V12722[a]	????????????0??????????????????????????????
Yamaceratops gobiensis	11??1010????1??????0101000101001010011011 1000
Prenoceratops peiganensis	??0?1???1?00101?000??0100?1110011??011?11????

	4444555555555566666666667777777777888888888 9 6789012345678901234567890123456789012345678 90
Hypsilophodon foxi	0001100--00000001?1000010000010001000000000 0
Stegoceras validus	0011100--0000000?00000?00?0001001000000 0?000
Archaeoceratops oshimai	??11??10???11101?01001110?1?10101 0??01?1110?1
Asiaceratops salsopaludalis	???????????11?00?????????1101??0?????001????
Bagaceratops rozhdestvenskyi	111????111011101001001111111110?011011111?111
Chaoyangsaurus youngi	0001?????????01?0???????1100?101001??0000000?1
Centrosaurus apertus	11100221 1?121101110112110211110?0101210110000?
Leptoceratops gracilis	111?10100001 1?10011010111121000101001101 10101
Graciliceratops mongoliensis	????????100?1?????????????????1?1??0??01?111???1
Montanoceratops cerorhynchus	?????0?0???112100??010?1????1?1??010011?11???1
Protoceratops andrewsi	1111?1211A01110100100111111111001011011111 0111
Psittacosaurus mongoliensis	01111010010010000010010000110110 00?01?0000001
Triceratops horridus	11100221011211011101121102111 10?0101210110001
Udanoceratops tshizhovi	?????????????????????????1??21?0??0?001?011??01
Zuniceratops christopheri	????????????1?????????????????11?1??0??0?????????
Liaoceratops yanzhiguouensis	00111010110011010?10011?00110011000 01?0101001
Psittacosaurus sinensis	????1?010010???????0???000011010 00??01?0000000?
IVPP V12722[a]	?????????????????????????????11010?1?????0?000?1
Yamaceratops gobiensis	00111010???111010?100111?1110001 0?00111111 0?1
Prenoceratops peiganensis	???????0???11210??????11?12100010??011011???1

APPENDIX 2
(*Continued*)

	1111111111111111111111111111111111
	9999999990000000000111111111122222222223333
	1234567890123456789012345678901234567890123
Hypsilophodon foxi	0000000000000000000000000000?00000000000000
Stegoceras validus	000000000000000??0?0?10?????00?0?0???01000
Archaeoceratops oshimai	0101000101???0?1000??0100?0??????????00??00
Asiaceratops salsopaludalis	??3-000?000?001??????????1????1???????????0
Bagaceratops rozhdestvenskyi	013-000201010011????1?????????????????0??????
Chaoyangsaurus youngi	111000000000000000000??????????????????????
Centrosaurus apertus	013-111201110111111212031011101011111111111
Leptoceratops gracilis	013-002211011011010111010111011000000000000
Graciliceratops mongoliensis	????000201010??????????1??1???1??????0??0000
Montanoceratops cerorhynchus	?1??002211011011011?11201110110?00000000000
Protoceratops andrewsi	011100020101001101111112011101100001000001
Psittacosaurus mongoliensis	003-000000000000000010000000?11100000000000
Triceratops horridus	013-111201110117111212031011101011111111111
Udanoceratops tshizhovi	013-002211011011??????02011??1100??????0???
Zuniceratops christopheri	???-0?120101?01??????????0?????????????1????
Liaoceratops yanzhiguouensis	010000100?10001?????????????????0???????????
Psittacosaurus sinensis	?03-00?0?000?000??0010?1000????10??????0?00
IVPP V12722[a]	111?000000000000000????0??????110????????0?0?
Yamaceratops gobiensis	01A000010001001??????0??1???????????????00
Prenoceratops peiganensis	013-002211011O?1??????????????????????????

[a]IVPP 12722 is a fragmentary species similar to Chaoyangsaurus (Zhao et al., in press).

APPENDIX 3

List of Anatomical Abbreviations

?	unidentified bone fragment
aep	articulation for epijugal
an	angular
aof	antorbital fossa
apd	articulation for predentary
bcp	basicranial pit
bo	basioccipital
bp	buccal process of rostral
cp	coronoid process of surangular
d	dentary
dp	dorsal process of rostral
ect	ectopterygoid
eoc	exoccipital
epi	epipterygoid
fm	foramen magnum
fr	frontal
gl	glenoid
gw	glenoid wall of surangular
idm	insertion for m. depressor mandibulae
itf	infratemporal fenestra
isp	ischial peduncle
j	jugal
je	jugal embayment
jp	jugal process of maxilla
la	lacrimal
las	lateral articular sulcus
lc	lateral condyle of quadrate
lsr	lateral surangular ridge
max	maxilla
mas	medial articular sulcus
mp	medial process of surangular
mps	palatal shelf of maxilla
opt	opisthotic
pa	parietal
pal	palatine
po	postorbital
pp	pubic peduncle
ppf	pterygopalatine fenestra
prf	prefrontal
pr	primary ridge on cheek teeth
prz	prezygapophysis
pt	pterygoid

ptw	pterygoid wing	rps	rostral process of surangular
pz	postzygapophysis	sa	surangular
q	quadrate	saa	surangular articulation for angular
qh	quadrate head	so	supraoccipital
qj	quadratojugal	sp	splenial
qjp	quadratojugal process of quadrate	sq	squamosal
rap	retroarticular process	sr2(5)	attachment scar for sacral rib 2 (or 5)
rp	rostral process	stf	supratemporal fenestra

Complete lists of all issues of the *Novitates* and the *Bulletin* are available at World Wide Web site http://library.amnh.org/pubs. Inquire about ordering printed copies via e-mail from scipubs@amnh.org or via standard mail from: American Museum of Natural History, Library—Scientific Publications, Central Park West at 79th St., New York, NY 10024. TEL: (212) 769-5545. FAX: (212) 769-5009.

♾ This paper meets the requirements of ANSI/NISO Z39.48-1992 (Permanence of Paper).